
138
078
THS

This is to certify that the
thesis entitled

A POTENTIAL-FLOW REACTOR MODEL FOR INITIAL DESIGN OF PULSE-PUMPED GROUNDWATER REMEDIATION SYSTEMS

presented by

CRAIG MICHAEL TENNEY

has been accepted towards fulfillment
of the requirements for the

M.S. degree in Chemical Engineering

R. Mark Worden
Major Professor's Signature

5/7/04
Date

A POTENTIAL-FLOW REACTOR MODEL FOR INITIAL DESIGN OF PULSE-PUMPED GROUNDWATER REMEDIATION SYSTEMS

By

Craig Michael Tenney

A THESIS

Submitted to
Michigan State University
in partial fulfillment of the requirements
for the degree of
MASTER OF SCIENCE

Department of Chemical Engineering and Materials Science

2004

ABSTRACT

A POTENTIAL-FLOW REACTOR MODEL FOR INITIAL DESIGN OF PULSE-PUMPED GROUNDWATER REMEDIATION SYSTEMS

By

Craig Michael Tenney

A computational model is presented for the optimization of pulsed pumping systems for efficient *in situ* remediation of groundwater contaminants. In the pulsed pumping mode of operation, periodic rather than continuous pumping is used. During the pump-off or trapping phase, natural gradient flow transports contaminated groundwater into a treatment zone surrounding a line of injection and extraction wells that transect the contaminant plume. Prior to breakthrough of the contaminated water from the treatment zone, the wells are activated and the pump-on or treatment phase ensues, wherein extracted water is augmented to stimulate pollutant degradation and recirculated for a sufficient period of time to achieve mandated levels of contaminant removal. An important design consideration in pulsed pumping groundwater remediation systems is the pumping schedule adopted to best minimize operational costs for the well grid while still satisfying treatment requirements. Using an analytic two-dimensional potential flow model, optimal pumping frequencies and pumping event durations have been investigated for a set of model aquifer-well systems with different well spacings and well-line lengths and varying aquifer physical properties. The flow model serves as a computationally efficient tool for initial design and selection of the pumping regimen best suited for pulsed pumping operation for a particular well configuration and extraction rate.

To the Unknown. May there always be something new to ponder.

ACKNOWLEDGMENTS

Thanks in particular go to Christian Lastoskie for much helpful support provided during the course of this research. The advice and information provided at various stages by Michael Dybas, David Hyndman, and David Wiggert is also very much appreciated. Support for this project was provided by the Michigan Department of Environmental Quality under contract Y40386 and the National Science Foundation under award CTS-9733086.

PREFACE

Chapters 1 and 2 are excerpted from two separate manuscripts. Although Chapter 2 is a logical extension of Chapter 1, each chapter was written to stand alone, and either chapter may be read independently of the other without loss of understanding or completeness.

TABLE OF CONTENTS

LIST OF TABLES vii

LIST OF FIGURES viii

CHAPTER 1
A Reactor Model for Trap-and-Treat Groundwater Remediation 1
Nomenclature 1
Introduction 3
Methodology 5
Results 12
Discussion 17
Conclusion 22
Tables 23
Figures 24

CHAPTER 2
Pulsed Pumping Process Optimization Using a Potential Flow Model 31
Nomenclature 31
Introduction 33
Methodology 36
Results 41
Discussion 44
Conclusion 51
Figures 53

REFERENCES 62

LIST OF TABLES

Table 1-1: Varied finite difference model parameters. 23

Table 1-2: Average measured hydraulic conductivity at 15-well site (Hyndman et al., 2000) 23

LIST OF FIGURES

Figure 1-1. (a) Injection, extraction, and recirculation zones for a two-well system. (b) Conceptual reactor network model for an arbitrary number of wells. The dashed box encloses subsurface flow within a single aquifer layer. Additional layers operate in parallel with the layer shown. 24

Figure 1-2. Streamlines and groundwater velocity contours for a single confined layer with $Q_e^* = 4.8$. The natural groundwater flow gradient is in the positive y-direction. (a) Two-well system with extraction well on the left and injection well on the right. (b) Staggered three-well system with two extraction wells and one injection well.. 25

Figure 1-3. Dimensionless residence time distribution $E^* = EL/V$ reported in terms of dimensionless time $t^* = tV/L$ for (a) two-well and (b) three-well systems with $Q_e^* = 9.6$ 26

Figure 1-4. Extraction zone concentration histories from FD simulation (solid squares) and from the reactor model (open squares) in a confined aquifer with two wells. (a) Conservative solute in a homogeneous aquifer with fully-screened wells. (b) Conservative solute in a heterogeneous aquifer with fully-screened wells. (c) Degradable solute in a homogeneous aquifer with fully-screened wells. (d) Conservative solute in a homogeneous aquifer with partially-screened wells. In part (d), the open squares and open diamonds show the reactor model results for 100% and 75% efficiency, respectively. 27

Figure 1-5. Measured and predicted tracer concentration histories for a 15-well field system. The experimental tracer measurements are shown as the solid squares; the reactor model results for 100% and 75% efficiency are given by the open squares and open diamonds, respectively. 28

Figure 1-6. Extraction zone solute concentration histories obtained for variation of key parameters. (a) Three-well system with $Q_e = 2.0$ m^3/hr and k = 0.20 (diamonds), 2.0 (squares), and 20. hr^{-1} (triangles); (b) Two-well (diamonds), three-well (squares) and five-well (triangles) systems with $Q_e = 2.0$ m^3/hr and k = 2.0 hr^{-1}; (c) Three-well system with k = 2.0 hr^{-1} and $Q_e = 8.0$ (diamonds), 2.0 (squares) and 0.50 m^3/hr (triangles). 29

Figure 1-7. (a) Effective recirculation zone width and (b) maximum allowable pump-off time as a function of pump-on time for trap-and-treat operation in a confined two-layer heterogeneous aquifer. The conductivities of the low- and high-conductivity layers are 0.075 and 0.15 m/hr, respectively. 30

Figure 2-1. Model aquifer structure and well geometry used for analysis of pulsed pumping. The geometric parameters for well length, well stagger, and aquifer layer

thickness are shown for a hypothetical five-well, three-layer system with vertical heterogeneity, as indicated by the layer-dependent specific discharge. 53

Figure 2-2. Streamlines obtained from potential flow model for an unstaggered, five-well system in a single confined aquifer layer with $Q^*=Q/(VHL)=30$ and an equal distribution of flow between all injection and extraction wells. If natural gradient groundwater flow is assumed to be in the positive y-direction, three wells are extracting groundwater and two wells are injecting. The recirculation zone is highlighted. 54

Figure 2-3. Allowable pump-off time to prevent contaminant breakthrough between pumping events for an arbitrary pulsed pumping system operating in a heterogeneous aquifer consisting of a low, medium, and high conductivity (K) layer. The allowable pump-off time is shown on the right axis as a function of the duration of each pumping event for the low (squares), intermediate (x's) and high (triangles) conductivity layers considered separately, and for the entire aquifer (solid line). The overall fraction of time the pumps are activated (dashed line) is shown on the left axis. 55

Figure 2-4. Dimensionless allowable pump-off time T^* versus dimensionless pump-on time t^* for single-layer systems. All combinations of $N = 5, 7, 9, 11, 13, 15, 21, 31, 45, 67, 99$ wells and dimensionless total pumping rates $Q^* = Q/(VHL) = 12, 20, 30, 50, 80, 120, 200, 300$ are represented (scattered +'s). $T^*=T[V(N\text{-}1)/(PRL)]$. $t^*=t[V(N\text{-}1)/(PRL)][6Q^*(N\text{-}1)/(\pi N)][1.948\exp(-0.694N)+0.0001081N+0.757]$. Note that T^* could equivalently be referred to as the recirculation zone width in units of L/(N-1). The data were fit to the equation $T^*=f(t^*)=0.5404(t^*\text{-}1)0.5292-0.0766(t^*\text{-}1)$ via least-squares regression (solid diamonds). The minimum of the $t^*/(t^*+T^*)$ curve (solid line) corresponds to the point of operation for maximally efficient pumping. Actual fractions of time spent with pumps on may be calculated from $t^*/(t^*+T^*)$ and the definitions of t^* and T^* 56

Figure 2-5. Total pumped volume required to flush a 15m deep x 15m long x 0.3m wide bioremediation zone versus the number of wells in the system. Values predicted by the potential flow model (connected diamonds) are compared with values calculated using a MODFLOW finite-difference groundwater flow model (solid squares, Hyndman et al. 2000). Values of V=0.356 m/week, P=0.3, and R=1 were applied to the potential flow model based upon the published aquifer characteristics..... 57

Figure 2-6. Pump-on times that minimize total pumping requirements for pulsed pumping systems operated in heterogeneous aquifers. Dimensionless pump-on time t* is plotted against the superficial velocity ratio $V^* = V_{max}/V_{min}$ for systems with various dimensionless total pumping rates $Q^*=Q/(VHL)$. Systems with $N = 7, 9, 11, 13, 15, 21, 31, 45, 67$, and 99 wells are represented. $t^*=t[1/V^*][V_{max}(N\text{-}1)/(PRL)][6Q^*(N\text{-}1)/(\pi N)][1.948\exp(-0.694N)+0.0001081N+0.757]$..... 58

Figure 2-7. Pump-off times that minimize total pumping requirements for pulsed pumping systems operated in heterogeneous aquifers. Dimensionless pump-off time

T^* is plotted against dimensionless total pumping rate Q^* for systems with various degrees of vertical heterogeneity, as measured by the superficial velocity ratio V^*. Systems with $N = 7, 9, 11, 13, 15, 21, 31, 45, 67$, and 99 wells are represented. $T^*=T[V(N-1)/(PRL)]$. 59

Figure 2-8. Minimum required fraction of time with pumps on for pulsed pumping systems operated in heterogeneous aquifers. The fraction of pump-on time resulting from use of the most efficient pulsed pumping schedule is plotted against dimensionless total pumping rate Q^* for systems with various degrees of vertical heterogeneity, as measured by the superficial velocity ratio V^*. Systems with $N = 3, 5, 7, 9, 11, 13, 15, 21, 31, 45, 67$, and 99 wells are represented. 60

Figure 2-9. Minimum possible average dimensionless total pumping rate for pulsed pumping systems operated in heterogeneous aquifers. The average dimensionless total pumping rate resulting from use of the most efficient pulsed pumping schedule is plotted against dimensionless total pumping rate Q^* for systems with various degrees of vertical heterogeneity, as measured by the superficial velocity ratio V^*. Average total pumping rate is the product of the fraction of pump-on time and the total pumping rate. Systems with $N = 3, 5, 7, 9, 11, 13, 15, 21, 31, 45, 67$, and 99 wells are represented. 61

CHAPTER 1

A Reactor Model for Trap-and-Treat Groundwater Remediation

Nomenclature

a	spatial coordinate of point source/sink	(m)
C	concentration	(mol/m^3)
D	well borehole or injection/extraction zone diameter	(m)
E	exit-age residence time distribution	(hr^{-1})
F	feed-normalized residence time distribution	(-)
H	aquifer layer thickness	(m)
k	degradation rate constant	(hr^{-1})
K	aquifer layer conductivity	(m/hr)
L	well line length	(m)
N	number of wells	(-)
P	porosity	(-)
Q	volumetric flowrate	(m^3/hr)
R	retardation factor	(-)
S	well line stagger (offset)	(m)
t	time	(hr)
v	fluid velocity	(m/hr)
V	natural gradient specific discharge	(m/hr)
w	complex potential function	(m^2/hr)
x	spatial coordinate perpendicular to natural gradient	(m)

y	spatial coordinate in the direction of natural gradient	(m)
z	complex spatial coordinate	(m)

Greek

Ψ	stream function	(m^2/hr)
τ	residence time	(hr)
Φ	velocity potential	(m^2/hr)

Subscripts

b	bypass stream
c	captured stream
d	discharge stream
e	extracted stream
i	injected stream
j	layer index
k	well index
m	midpoint of timestep
r	recirculated stream

Introduction

Trap-and-treat remediation refers to the use of periodic rather than continuous pumping for the capture and degradation of groundwater contaminants. During the pump-off phase of the trap-and-treat approach, contaminants are transported by natural gradient groundwater flow into an adsorption zone proximate to a transect of alternating injection and extraction wells. Contaminant adsorbs onto aquifer solids in this region until near saturation is attained, whereupon the well pumps are activated to establish recirculation between adjacent injection and extraction wells. The recirculation zone is then flushed with augmented water to stimulate chemical or biological degradation of the adsorbed contaminant. Once the zone has been cleansed of contaminant, the pumps are shut off, allowing fresh contaminant to adsorb onto the aquifer solids from the next parcel of groundwater that enters the treatment zone by natural gradient flow. The alternating sequence of *pump-off* (contaminant adsorption) and *pump-on* (contaminant degradation) events is continued for the duration of the treatment project.

A hybrid scheme involving bioaugmentation and trap-and-treat operation has been developed for the *in-situ* bioremediation of Schoolcraft Plume A, a carbon tetrachloride plume in an unconfined aquifer in southwest Michigan (Dybas *et al.*, 1998). Bioaugmentation of Plume A with *Pseudomonas stutzeri* strain KC, a non-native microorganism, enables transformation of carbon tetrachloride into carbon dioxide and other nonvolatile organic compounds without production of chloroform (Criddle *et al*, 1990; Dybas *et al.*, 1995). By contrast, biostimulation of indigenous Plume A microflora results in substantial chloroform production (Mayotte *et al.*, 1996). Trap-and-treat operation was implemented for a fifteen-well plume transect at the Schoolcraft site, with

weekly pumping events interrupting passive adsorption of carbon tetrachloride from the groundwater onto the aquifer solids in the treatment zone. Over a 1550-day field test (Dybas *et al.*, 2002), more than 96% of the adsorbed carbon tetrachloride was transformed with minimal production of chloroform. A well-designed trap-and-treat system may allow significant cost savings relative to continuous pump-and-treat remediation systems, which typically have relatively high maintenance costs and require pumping and disposal of large volumes of water (Dybas, personal communication).

To achieve maximum effectiveness from trap-and-treat remediation, the placement of injection/extraction wells and the pumping schedule must be judiciously chosen. In this paper, we present a reactor model that has been developed for use as a computationally efficient trap-and-treat design optimization tool. This model is primarily intended for use in the early stages of system design, when detailed aquifer properties are not likely known, to rapidly evaluate a large range of potential system configurations. For comparison with trap-and-treat systems, the model can also predict the transient and steady state behavior of continuously-pumped remediation systems, which are fundamentally equivalent to pulsed systems with infinite pump-on times. The reactor model is largely analytic and is thus resource efficient in comparison to numerical model packages such as MODFLOW (McDonald and Harbaugh, 1983) and MT3D (Zheng, 1992).

Methodology

The aquifer is divided into laterally homogeneous layers with specific hydraulic conductivities. The reactor model partitions each aquifer layer into injection, extraction, and recirculation zones, as depicted in Figure 1-1(a) for a two-well system. The injection and extraction well casings are enclosed by circular regions of diameter D equal to the well borehole diameter. Ideal radial plug flow is assumed in the injection and extraction zones. The recirculation zone is defined as the region between adjacent wells through which pumped water flows from the injection zone to the extraction zone. Plug flow does not occur in this region, but rather a distribution of fluid velocities and residence times is presumed.

Each of the three zones within an aquifer layer is modeled as a separate chemical reactor, as indicated in Figure 1-1(b) for a single layer aquifer. For multiple layer aquifers, with physical properties that vary across layers, vertical dispersion is neglected, such that the recirculation zones of the layers operate in parallel and flow and reaction in each layer occur independently of the other layers. The outflows from the recirculation zones combine and mix completely within a single extraction zone that vertically spans all layers. Similarly, the injection zone is completely mixed, so that the injected fluid composition is the same in all layers.

For systems of more than two wells, there are multiple injection, extraction, and recirculation zones within each aquifer layer. For computational efficiency these zones are mathematically combined into single injection, extraction, and recirculation reactor units that collectively represent the total flow and reaction occurring within a given layer. This simplification is possible without loss of generality in the final results because

reaction and flow in the injection, extraction, and recirculation zones are modeled according to residence time distributions rather than spatial location.

Assuming the diameter of the well casing is negligible relative to the borehole diameter, the solute residence time τ for radial plug flow in the injection zone and the extraction zone is

$$\tau = \pi D^2 PRH/(8Q_e) \quad (1)$$

where Q_e/H is the volumetric extraction rate per unit layer thickness for a given well; P is the porosity; and R is the retardation factor for the solute in question assuming equilibrium linear adsorption.

The boundaries of the recirculation zone within a given layer and the fluid residence time distribution within this zone depend upon the well configuration and spacing and the pumping extraction rate Q_e. For very low values of Q_e, the extraction rate is insufficient to establish recirculation between adjacent wells, and the bypass flowrate Q_b of incoming fluid not captured by the extraction well is nonzero. For larger extraction rates that represent typical pumping conditions, all incoming groundwater is captured ($Q_b = 0$), and the recirculation zone volume and its associated residence time distribution (RTD) are calculated using an analytic two-dimensional potential flow model (Bird *et al.*, 1960; Columbini, 1999).

The potential flow model assumes steady-state, continuous, incompressible, inviscid, irrotational, two-dimensional flow occurs within homogeneous, isotropic layers of a confined aquifer. The natural gradient groundwater flow or specific discharge V is in the positive direction along the y-coordinate. A set of N injection/extraction wells are evenly spaced along a line of length L in the x-coordinate, with perpendicular stagger S

between consecutive wells. Sample configurations for two- and three-well systems are shown in Figure 1-2. All wells are assumed to be fully screened ideal sources or sinks.

Continuity and irrotational flow require that

$$\frac{\delta v_x}{\delta x} + \frac{\delta v_y}{\delta y} = 0 \tag{2}$$

$$\frac{\delta v_x}{\delta y} - \frac{\delta v_y}{\delta x} = 0 \tag{3}$$

where v_x and v_y are the rectangular components of the fluid velocity. A solution may be obtained in terms of the stream function Ψ and velocity potential Φ, which are combined into the complex potential $w(z)$, where $z = x + i\,y$:

$$w(z) = \Phi(x,y) + i\,\Psi(x,y) \tag{4}$$

$$v_x = -\frac{\partial \Psi}{\partial y} = -\frac{\partial \Phi}{\partial x} \tag{5}$$

$$v_y = +\frac{\partial \Psi}{\partial x} = -\frac{\partial \Phi}{\partial y} \tag{6}$$

For a single layer, two-well system with an injection rate $+Q_e/H$ at $z = +L/2$ and extraction rate $-Q_e/H$ at $z = -L/2$ superimposed on the specific discharge, the complex potential reported in terms of the dimensionless pumping rate $Q_e^* = Q_e/(HLV)$ is

$$w^*(z^*) = \frac{Q_e^*}{2\pi} \ln\left(\frac{z^* - 1/2}{z^* + 1/2}\right) + iz^* \tag{7}$$

where $z^* = z/L$ and $w^* = w/(LV)$. For a single layer, N-well system with even-numbered extraction wells staggered a distance S in the $+y$ direction behind odd-numbered injection wells along a line of length L, the complex potential is

$$w^*(z^*) = \sum_{k=1}^{N} \frac{Q_{ek}^*}{2\pi} \ln\left(z^* - a_k^*\right) + iz^* \tag{8}$$

$$Q_{ek}{}^{*} = \begin{cases} \dfrac{Q_e{}^{*}}{\text{int}\left[(N+1)/2\right]}, & k \text{ odd} \\ -\dfrac{Q_e{}^{*}}{\text{int}\left[N/2\right]}, & k \text{ even} \end{cases} \tag{9}$$

$$a_k{}^{*} = \begin{cases} \left(-\dfrac{1}{2} + \dfrac{k-1}{N-1}\right) + i\dfrac{S^{*}}{2}, & k \text{ odd} \\ \left(-\dfrac{1}{2} + \dfrac{k-1}{N-1}\right) - i\dfrac{S^{*}}{2}, & k \text{ even} \end{cases} \tag{10}$$

where int[x] is the truncated integer value of x and $S^{*} = S/L$. Equation (9) stipulates that the total volumetric flowrate $Q_e{}^{*}$ is distributed equally across the extraction wells and injection wells; e.g. for a five-well system with $S^{*} = 1$, groundwater is extracted at a rate $-Q_e{}^{*}/2$ from wells 2 and 4 at coordinates $a_2{}^{*} = (-1/4, -i/2)$ and $a_4{}^{*} = (+1/4, -i/2)$, and injected at a rate $+Q_e{}^{*}/3$ from wells 1, 3 and 5 at coordinates $a_1{}^{*} = (-1/2, +i/2)$, $a_3{}^{*} = (0, +i/2)$, and $a_5{}^{*} = (+1/2, +i/2)$.

For an N-well system in an M-layer heterogeneous aquifer, the dimensionless complex potential $w_j{}^{*} = w/(LV_j)$ in layer j is the same as that given by equations (8-10), except that the dimensionless pumping rate in equation (9) is

$$Q_e{}^{*} = \frac{Q_e}{L\sum_{j=1}^{M} H_j V_j} \tag{11}$$

where H_j and V_j are the respective thickness and specific discharge of the j^{th} layer. The velocity field $v_j(z)$ of layer j is obtained from the derivative of the complex potential:

$$v_j(z) = \frac{dw_j}{dz} = V_j \sum_{k=1}^{N} \frac{Q_{ek}{}^{*}}{2\pi} \frac{1}{\left(z^{*} - a_k{}^{*}\right)} + iV_j \tag{12}$$

where the x- and y-components of the velocity are given as the real and imaginary portions of equation (12), respectively.

Figure 1-2(a) shows the flow streamlines and groundwater velocity contours calculated for a two-well system with $Q_e^* = 4.8$. Figure 1-2(b) shows the results for a staggered three-well system with the same pumping rate. Each well has a corresponding stagnation point, indicated by the dark contours of Figures 2(a) and (b). The difference in stream function values calculated at the stagnation points of consecutive wells is used to determine the groundwater capture rate Q_c and the recirculation flowrate $Q_r = Q_e - Q_c$ for each well (or well pair) in the trap-and-treat system. A similar approach has been used to delineate well capture zones in two-dimensional groundwater flow models (Bakker *et al.*, 1996).

The recirculation zone is modeled as a segregated flow reactor (Levenspiel, 1999; Fogler, 1999) in which a set of plug flow reactors (PFRs) with a distribution of residence times operate in parallel. The residence time distribution (RTD) of the segregated flow reactor is determined from the fluid streamlines in the recirculation zone obtained for a given well geometry and pumping rate.

The PFR reactor network shown in Figure 1-1(b) permits analytic solution of the contaminant concentration versus time at any point within the network once the initial conditions (i.e. C_e, C_i, and C_r in Figure 1-1(b) at t=0), aquifer physical properties, kinetic parameters, and well geometry and pumping rates are specified. The solute concentration C_c of incoming captured groundwater is assumed constant within a given layer. Equilibrium linear adsorption and first order reaction are also assumed, with a degradation rate constant k specific to each reactor unit.

For first-order reaction, the contaminant concentration $C_i(t)$ exiting the radial PFR that represents the injection zones is obtained from the concentration $C_e(t)$ entering this zone as:

$$C_i(t) = C_e(t-\tau)\exp(-k\tau) \tag{13}$$

where τ is given by equation (1). Similarly, for the extraction zone:

$$C_e(t) = [\,(Q_c/Q_e)C_c + (Q_r/Q_e)C_r(t-\tau)\,]\exp(-k\tau) \tag{14}$$

The outlet concentration from the recirculation zone is given by the convolution integral

$$C_r(t) = \int_0^\infty E(\tau)C_i(t-\tau)\exp(-k\tau)\mathrm{d}\tau \tag{15}$$

where the residence time distribution $E(\tau)$ is calculated using a second-order numerical particle-tracking algorithm. This is the only non-analytic calculation performed in solving the reactor model. A selected number of particles are uniformly distributed around the circumference of the injection well. The trajectory of each particle is tracked forward in time until it either reaches an extraction well or it moves beyond a specified distance (i.e. along a streamline outside of the recirculation zone; these particles are discarded in the RTD analysis). The particle location at the end of the next timestep is calculated from its current position and the analytic velocity field as

$$z^*(t+\Delta t) = z^*(t) + [\,v_m^*/|v_m^*|\,]\,\Delta t \tag{16}$$

$$v_m^* = v^*(\,z^* + \tfrac{1}{2}\,[\,v^*(z^*)/|v^*(z^*)|\,]\,\Delta t) \tag{17}$$

where Δt is the time increment and the dimensionless velocity $v^*(z^*) = -v_x/V + \mathrm{i}v_y/V$ at the dimensionless spatial coordinate z^*. Figure 1-3 shows the particle travel time distributions for two- and three-well systems with $Q_e^* = 9.6$ in which the effects of porosity and retardation are neglected. The travel time distribution is multiplied by the

porosity and retardation factor to yield $E(\tau)$ for the recirculation zone. The integral of equation (15) is then discretized to obtain the exit concentration from the recirculation zone.

Once initial conditions are specified, the time-dependent concentrations C_e, C_i, and C_r are solved using $E(\tau)$ for the specified well geometry and pumping rate by combining equations (13)-(15) into one equation with t as the only unknown. The extraction well concentration C_e is typically of interest to compare against groundwater field measurements, whereas the discharge concentration

$$C_d = (Q_c/Q_d)C_i + (Q_b/Q_d)C_c \tag{18}$$

where $Q_d = Q_c + Q_b$, is relevant in regard to regulatory compliance.

Results

Transport tests with conservative tracers and reactive solutes were simulated using the reactor model and the results were compared with calculations from a three-dimensional finite difference (FD) MODFLOW/MT3D model using a 10 m × 10 m × 6 m grid with a grid spacing of 0.1 m in the lateral (x- and y-) coordinates. Advection within the FD model is simulated using a fourth-order Runge-Kutta hybrid method of characteristics solution algorithm. The simulated trap-and-treat system consists of one-meter diameter reactive (injection/extraction) zones around two wells spaced two meters apart within a six-meter thick confined aquifer that is assumed to be initially free of solute. Transient solute concentrations are calculated for a hypothetical ten-hour pumping interval with constant injection concentration C_i = 100 ppm. Results for single-layer and three-layer aquifers are compared for the model systems listed in Table 1-1. The following invariant parameter values were used in the finite difference simulations: porosity = 0.3, dispersivity = 0.1 m, head gradient = 0.01, and leakance between layers = 0.01 hr^{-1}.

Figure 1-4(a) shows the extraction well concentration C_e predicted for a conservative tracer in a homogeneous, single-layer confined aquifer. Tracer extraction begins after approximately two hours in the FD model, and after 3.5 hours in the reactor model. The difference is due to longitudinal dispersion, which is accounted for in the FD model but neglected in the reactor model. After approximately four hours, the extracted tracer concentrations predicted by the reactor model are very close to those of the FD model. The inability of the reactor model to simulate early, low concentration, dispersion-induced breakthrough of solute is not expected to limit the model's utility

because pulse-pumped systems are not generally expected to use such relatively short pump-on times. Simulations with three-layer, homogeneous FD and reactor models yielded similar results as those shown in Figure 1-4(a) and are not presented here.

Figure 1-4(b) shows FD and reactor model simulation results for a conservative tracer in a three-layer, heterogeneous confined aquifer in which the top and bottom aquifer layers have a lower conductivity than the middle layer. The combined pumping rate Q_e for the three layers matches the pumping rate for the case shown in Figure 1-4(a). The tracer breakthrough times for the FD and reactor models agree more closely for the heterogeneous aquifer of Figure 1-4(b) than for the homogeneous aquifer of Figure 1-4(a). It appears that neglect of longitudinal dispersion in the reactor model becomes less significant as heterogeneity is added to the system and dispersion effects are spread across several layers. The extraction well concentration curves are again in good agreement at later times.

Figure 1-4(c) shows FD and reactor model simulation results for a reactive solute in a single-layer confined aquifer with fully-screened wells. This case is identical to that of Figure 1-4(a), except that solute degradation with first-order kinetics occurs within the aquifer. It is again observed that the reactor model predicts a longer breakthrough time than the FD model, due to neglect of dispersion, whereas agreement between the models at later times is quite good.

Figure 1-4(d) shows a comparison of the FD and reactor models for a conservative tracer in a confined aquifer with partially-screened wells. The FD model is comprised of three layers, with a well screen present only in the middle layer, so that groundwater can only be injected and extracted from this layer and not the others. The

reactor model results of Figure 1-4(d), meanwhile, are reported only for the layer in which the well screen is present. The solute concentration curves predicted by the FD and reactor models in Figure 1-4(d) differ significantly. As in the previous cases, the two models predict different tracer breakthrough times due to the effect of dispersion. More significant is that the reactor model overestimates the extraction well concentration at longer pumping times. There are two reasons for this. First, solute arrival is delayed because some fluid streamlines in the three-dimensional FD flow model are able to travel through the unscreened layers, which results in residence times longer than predicted by the two-dimensional analytic solution used in the reactor model. Second, the addition of unscreened layers above and below the recirculation zone FD model allows for greater solute loss due to dispersion from the recirculation zone. The reactor model curve in Figure 1-4(d) labeled 100% efficiency assumes, as in Figures 4(a-c), that no solute is lost from the recirculation zone. The reactor model curve labeled 75% efficiency in Figure 1-4(d) is obtained if one assumes that 25% of the solute entering the recirculation zone is permanently lost to dispersion before it reaches the extraction well. With this empirical adjustment, the reactor model predictions can be brought into close agreement with the FD model results for times out to ten hours. Although not shown, a 90% efficiency factor provides a better fit when steady state is achieved near 100 hours, suggesting that only 10% of the solute is actually lost to dispersion and providing an estimate of the degree to which the remaining solute took a longer-than-predicted average path. Further study is needed to determine the extent to which model predictions vary as actual system properties depart from those assumed in the model. Recalling that this model is primarily intended to rapidly and efficiently evaluate a large number of potential operational

configurations during the early stages of system design when detailed aquifer properties may not be known, application of an empirical adjustment based upon prior experience to account for non-idealities should still provide conceptually useful results.

The FD and reactor model calculation times on a 400 MHz Intel Celeron processor are shown for ten hours of simulated pumping for each case in Table 1-1. The reactor model possesses a significant computational advantage relative to the FD model, which enables more rapid investigation of well geometries or changes in aquifer physical properties.

The aquifer at the Schoolcraft Plume A site is composed primarily of sand and gravel glaciofluvial sediments with significant vertical heterogeneity. A regional layer of clay exists approximately 27 meters below ground surface (bgs), and the water table is approximately 4.5 meters bgs (Hyndman *et al.*, 2000). A trap-and-treat system of fifteen wells arranged in a line fifteen meters long with no stagger was installed and screened from 9.1 to 24.4 meters bgs. Table 1-2 lists the average hydraulic conductivities for three-meter thick layers from 9 to 27 meters bgs as measured from well cores collected during installation of the system. A hydraulic head gradient of 0.0011, based on regional measurements, was used to calculate specific discharge for each layer.

During an initial tracer study, groundwater was extracted from odd-numbered wells at a total rate of 9.1 m^3/hr and injected into even-numbered wells for a period of five hours. Sodium bromide was added continuously to the injected groundwater to bring the average injected bromide concentration to 16 ppm. Bromide concentration was measured at each extraction well at thirty-minute intervals. Figure 1-5 shows the average extracted bromide concentration during the five-hour tracer test. The error bars denote

one standard deviation of the concentrations measured across the eight extraction wells. Variations in extracted concentration among the individual wells at any given time are primarily due to a combination of heterogeneity between the wells and variations in well spacing. A five-layer aquifer reactor model was developed using the physical property data of Table 1-2 and assuming an aquifer porosity of 0.3. The predictions of the reactor model are compared to the experimental tracer data in Figure 1-5. As in Figure 1-4(d), for 100% recirculation efficiency the reactor model overstates the extracted bromide concentration, but at 75% recirculation efficiency a good fit to the experimental data is obtained. The difference between the model predictions and field tracer measurements is primarily attributed to the assumption of fully-screened wells in the reactor model.

Comparison of the reactor model and FD predictions indicates that the reactor model yields quantitative predictions of the extracted solute concentration over intermediate to long timescales, provided that the assumption of full well screening in a confined aquifer is met. When the reactor model is applied to partially-screened well systems in confined or unconfined aquifers, the solute breakthrough curves are qualitatively similar to FD model results and experimental data, but a scaling factor that accounts for the effect of partial-screening is required to achieve quantitative agreement.

Discussion

The effect of the reaction rate constant, well density, and pumping rate on the extraction well contaminant concentration is shown in Figures 6(a), 6(b) and 6(c) respectively. The results reported in Figures 6(a-c) are for a two-meter line of unstaggered wells in a single confined layer with C_c = 100 ppm; V = 0.001 m/hr; P = 0.3; H = 6 m; and D = 0.30 m. Degradation is assumed to occur only in the injection and extraction zones, and retardation due to adsorption is neglected. For systems with an odd number of wells, the end wells are operated as extraction wells. The initial contaminant concentration in all zones is 100 ppm.

Figure 1-6(a) shows the sensitivity of the extracted solute concentration to changes in the first order degradation rate constant for a three-well system with Q_e = 2.0 m^3/hr. For k = 2.0 hr^{-1}, approximately 50% of the solute is degraded with each pass through the reactor network. This value of the rate constant is comparable to that measured for CT degradation by strain KC (Dybas *et al.*, 1995). As might be expected, changing the rate constant by an order of magnitude in Figure 1-6(a) significantly alters both the steady-state extraction well solute concentration and the rate of approach to the steady-state condition.

Figure 1-6(b) shows how the extracted groundwater solute concentration changes as the number of wells is varied while the well-line length is held constant. Increasing the well density increases the groundwater retention time within the injection and extraction zones, because the total volumetric flow is divided among a greater number of wells. The higher well density also increases the fraction Q_r/Q_e of injected groundwater that is recirculated. The higher recirculation ratio leads to longer overall retention times

and lower steady-state concentrations. The increased degradation efficiency afforded by a high well density is achieved, however, at the expense of a higher well installation cost per unit well-line length.

Figure 1-6(c) shows the effect of varying the pumping rate on the extracted solute concentration for a three-well system with a degradation rate constant of 2.0 hr^{-1}. Increasing the groundwater extraction rate has two competing effects. The recirculation ratio Q_r/Q_e increases as the pumping rate increases, resulting in longer overall retention times within the system. As the extraction rate increases, however, the fluid residence time in the injection and extraction zones decreases, so that the amount of degradation per fluid pass decreases at high pumping rates. For the three-well system of Figure 1-6(c), the effect of the shorter reactive zone residence time negates the benefit of increased recirculation, so that high pumping rates result in low degradation efficiency (i.e. C_e values). Furthermore, since operating costs increase as the total pumping burden increases, there is an economic disincentive to operating at very high extraction rates.

For very low pumping rates, much lower than those shown in Figure 1-6(c), the bypass flowrate Q_b becomes nonzero, and the overall degradation efficiency decreases due to the uncaptured groundwater fraction. Thus, there is an optimum intermediate pumping rate, dependent on the number and configuration of wells, that maximizes overall degradation of the contaminant.

In order to minimize total pumping costs, the pumping schedule for trap-and-treat operation should provide the largest possible ratio of pump-off time to total pumped groundwater volume. The principal trap-and-treat operating constraint is that the breakthrough of contaminant in the recirculation zone during the pump-off phase is

prohibited. Specific trap-and-treat remediation systems may have additional constraints; for example, the microorganisms in an *in situ* bioremediation system may require scheduled delivery of nutrients by pumping.

An estimate of the allowable pump-off time, as a function of the pump-on treatment time, can be obtained from the recirculation zone RTD in each aquifer layer. Assuming that uncontaminated and/or nutrient enriched water is continuously injected during the pump-on phase, the fraction of the recirculation zone volume in each layer that is fully swept by injected water is equal to the value of the feed-normalized RTD, $F(t)$, for pumping time t

$$F(t) = \int_0^t E(\tau)d\tau \tag{19}$$

This is equivalent to calculating the volume traversed by streamlines in the recirculation zone that arrive at the extraction well within the interval t. Dividing the swept volume by the well spacing and aquifer layer thickness yields an estimate of the swept recirculation zone width. The allowable pump-off time for a given layer is the time required for a parcel of groundwater traveling at the natural gradient velocity to cross this width.

Figure 1-7 shows the recirculation zone width and maximum pump-off time for a heterogeneous, two-layer, two-well aquifer, assuming negligible dispersion, chemical reaction, and adsorption. For continuous pumping, all aquifer layers have the same recirculation zone width, irrespective of their conductivities; but for intermittent pumping, the recirculation zone width increases more rapidly with pump-on time for the higher conductivity layer, as shown in Figure 1-7(a). The maximum time interval between pumping events that avoids solute breakthrough in each layer is shown in Figure 1-7(b). For short pump-on time, breakthrough during the pump-off phase occurs first in

the lower conductivity layer, because the swept width of the recirculation zone in this layer is narrower than in the higher conductivity layer. In fact, for pumping durations of less than 7.5 hours, the width of the swept region is zero in the lower conductivity layer, because there is insufficient time for injected groundwater to reach the extraction well.

For long pump-on times (e.g. $\tau = 15$ hours), the allowable pump-off time becomes greater for the lower conductivity layer. Although the swept width of the recirculation zone is always larger in the high conductivity layer, natural gradient flow is sufficiently slower in the lower conductivity layer so that it takes longer for a parcel of groundwater to cross the swept width of this layer. The crossover point, at which both layers have the same breakthrough time, occurs at a pump-on interval of eleven hours for the particular two-layer aquifer investigated in Figure 1-7.

If no contaminant is to be allowed to exit the swept portion of the recirculation zone during the pump-off phase, then the trap-and-treat system must be operated such that the interval between pumping events does not exceed the shortest of the allowable pump-off times for each aquifer layer; e.g. in Figure 1-7(b), a pump-off or "trapping" interval of 18 days for each pump-on or "treatment" period of 20 hours. Under this constraint, maximum trap-and-treat efficiency is achieved by operating at the point of crossover in the pump-off curves; i.e. in Figure 1-7(b), by adopting a schedule of eleven hours of pumping once every twelve days. Pump-on times shorter than this duration are disadvantageous because rapid breakthrough in the swept zone of the lower conductivity layer compels more frequent pumping. Pump-on times longer than the optimum eleven-hour duration, meanwhile, are also disadvantageous because the benefit of the longer pump-off time interval is negated by a disproportionately larger increase in the total

pumping burden incurred due to the longer pump-on time. For well configurations and for aquifers with physical properties that are different from the two-well, two-layer case considered in Figure 1-7, the preceding analysis will of course yield a different preferred pumping scheme. However, the same process optimization considerations will apply.

If solute adsorption is significant during both phases of operation, the swept recirculation zone width increases more slowly over time, and the allowable pump-off time increases. The curves of Figure 1-7(a) will then shift rightward, and those of Figure 1-7(b) rightward and upward, by an amount proportional to the retardation factor. In Figure 1-7(b), it was assumed that no reaction occurs between pumping events, but if solute degradation does occur during the pump-off phase, the maximum pump-off time again increases and the curves of Figure 1-7(b) shift upward. Also, the results shown in Figure 1-6 indicate that for certain conditions, the pumps must remain activated for a period of time before the injected water becomes sufficiently "clean", i.e. the discharge concentration attains its desired or steady-state concentration. In such cases, a longer pumping time is required to effectively sweep the recirculation zone, and the curves of Figures 7(a) and 7(b) shift rightward by an amount equal to the period of time needed to achieve the desired discharge concentration.

Conclusion

The two-dimensional flow, recycle reactor model presented in this work is intended as a tool for rapid initial design and analysis of trap-and-treat remediation systems. The model predicts transient and steady-state solute concentrations for different configurations of intermittently pumped field treatment systems. Comparisons with three-dimensional FD model calculations demonstrate that the reactor model accurately predicts solute transport in systems with first-order reaction, fully-screened wells, and heterogeneous layers when dispersion is not significant. The reactor model predictions also compare reasonably well with tracer breakthrough measurements from field experiments conducted at the Schoolcraft Plume A site. Extension of the reactor model to include multiple solutes and phases, and to incorporate more complicated kinetics and adsorption equilibria, is possible at the expense of computational speed. The semianalytic reactor model is computationally efficient for optimization of well spacing and geometry, pump extraction rate, and pumping schedule for trap-and-treat operations. For process modeling of aquifers with significant lateral dispersion or vertical flow, a fully three-dimensional approach using FD or other numerical methods is recommended.

Additionally, the reactor model provides a simple framework for thinking about relationships between remediation system behavior and general changes in aquifer properties, well configuration, and pumping rate and schedule. Future research will illustrate some of these relationships, which might not be readily apparent when working with conventional finite difference groundwater flow models, and provide dimensionless correlations for use in initial design studies.

Tables

Table 1-1: Varied finite difference model parameters.

Model	Figure	Layer	H (m)	K (m/hr)	Q_e (m^3/hr)	Computational time (s)	
						FD model	Reactor model
Homogeneous	1-4a	1	6	0.1	2	450	9
Heterogeneous	1-4b	1	2	0.075	0.5	2670	10
		2	2	0.15	1		
		3	2	0.075	0.5		
Reactive $k = 0.2\ hr^{-1}$	1-4c	1	6	0.1	2	420	9
Partial Screen	1-4d	1	2	0.1	-	1580	9
		2	2	0.1	0.67		
		3	2	0.1	-		

Table 1-2: Average measured hydraulic conductivity at 15-well site (Hyndman et al., 2000)

Depth (m)	9-12	12-15	15-18	18-21	21-24	24-27
Number of measurements	41	35	44	33	41	26
Average (cm/s)	0.012	0.012	0.027	0.023	0.046	0.057
Standard Deviation	0.006	0.003	0.011	0.013	0.024	0.022
Coefficient of Variation (%)	53	25	40	54	53	38

Figures

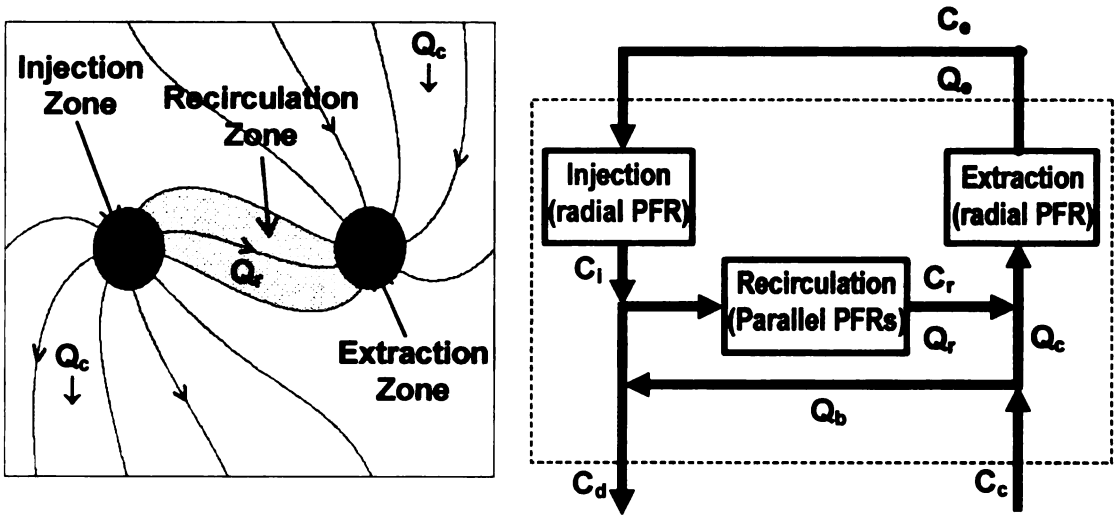

Figure 1-1. (a) Injection, extraction, and recirculation zones for a two-well system. (b) Conceptual reactor network model for an arbitrary number of wells. The dashed box encloses subsurface flow within a single aquifer layer. Additional layers operate in parallel with the layer shown.

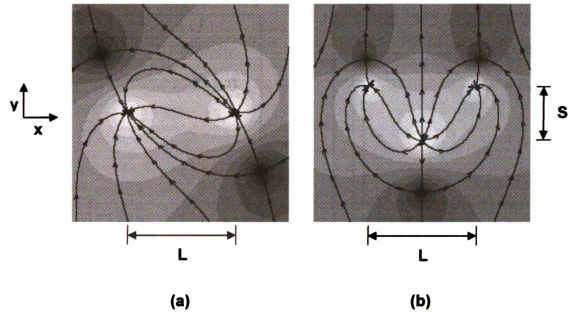

Figure 1-2. Streamlines and groundwater velocity contours for a single confined layer with $Q_e^* = 4.8$. The natural groundwater flow gradient is in the positive y-direction. (a) Two-well system with extraction well on the left and injection well on the right. (b) Staggered three-well system with two extraction wells and one injection well.

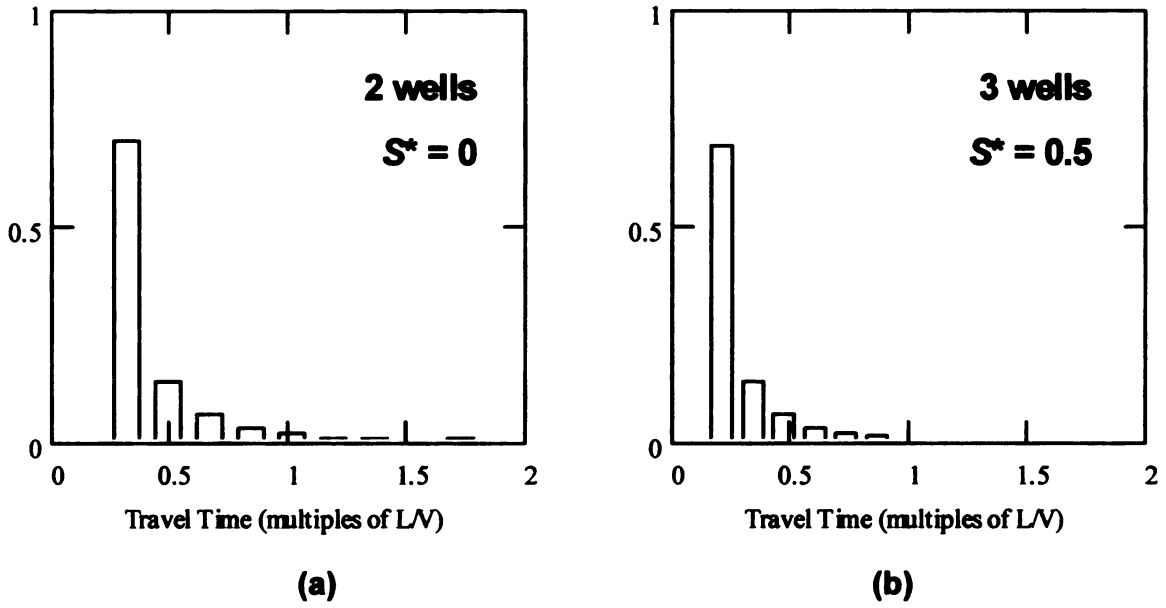

Figure 1-3. Dimensionless residence time distribution $E^* = EL/V$ reported in terms of dimensionless time $t^* = tV/L$ for (a) two-well and (b) three-well systems with $Q_e^* = 9.6$.

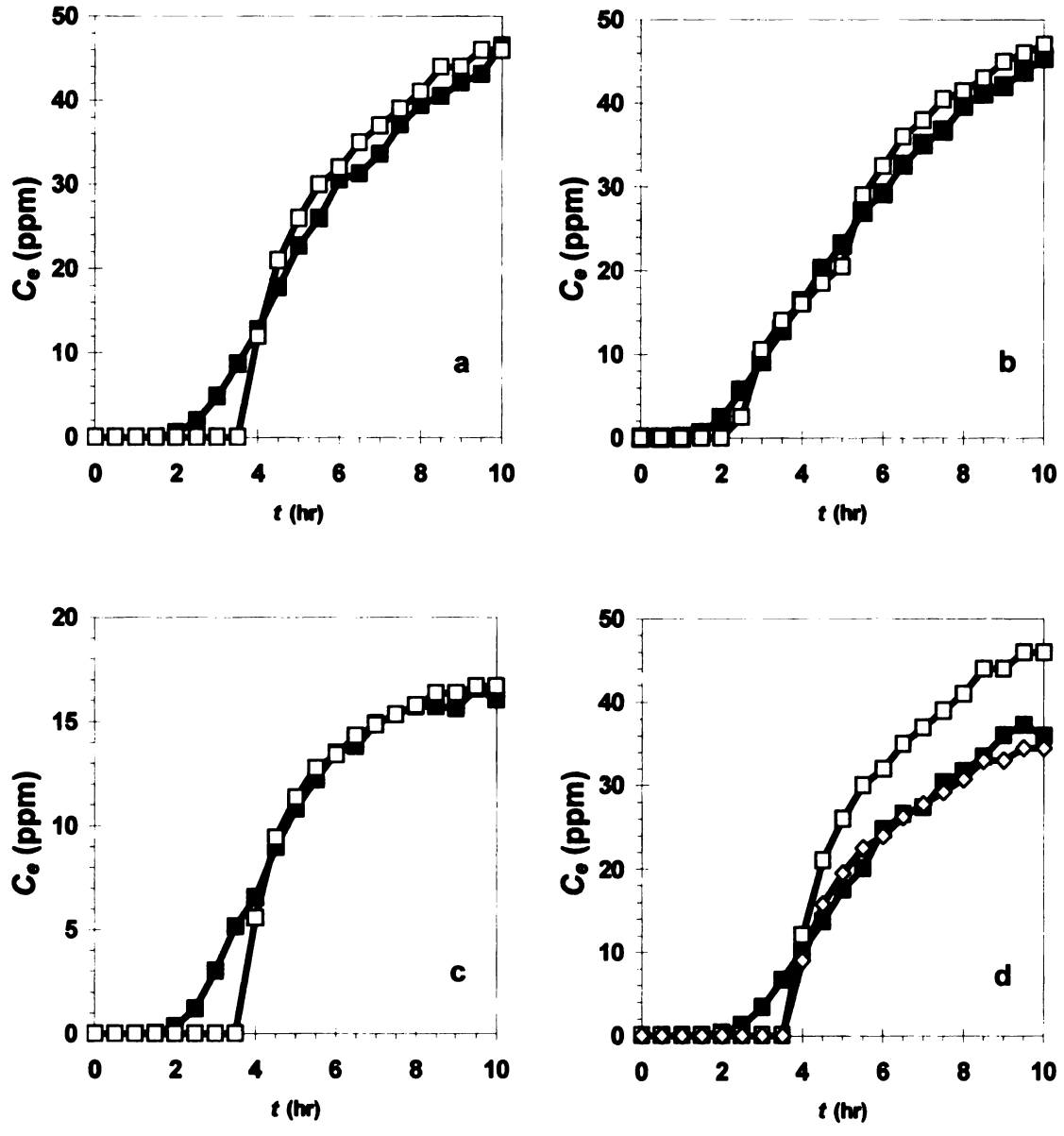

Figure 1-4. Extraction zone concentration histories from FD simulation (solid squares) and from the reactor model (open squares) in a confined aquifer with two wells. (a) Conservative solute in a homogeneous aquifer with fully-screened wells. (b) Conservative solute in a heterogeneous aquifer with fully-screened wells. (c) Degradable solute in a homogeneous aquifer with fully-screened wells. (d) Conservative solute in a homogeneous aquifer with partially-screened wells. In part (d), the open squares and open diamonds show the reactor model results for 100% and 75% efficiency, respectively.

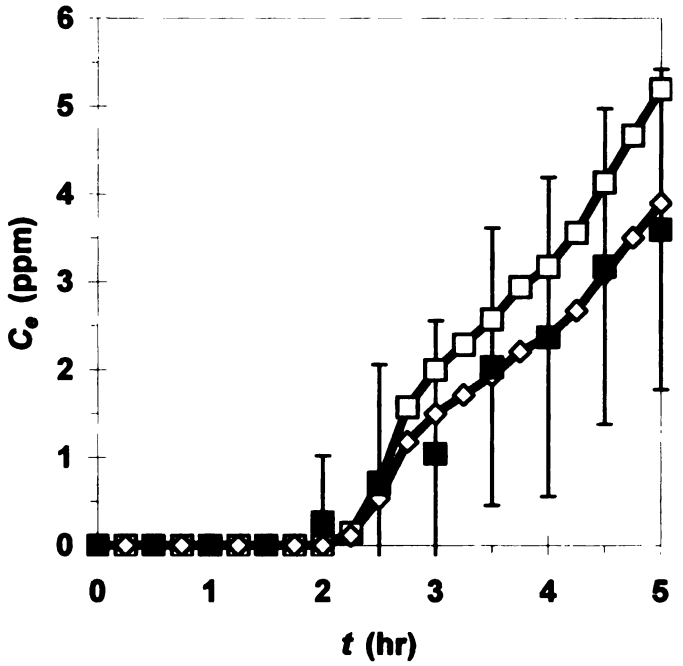

Figure 1-5. Measured and predicted tracer concentration histories for a 15-well field system. The experimental tracer measurements are shown as the solid squares; the reactor model results for 100% and 75% efficiency are given by the open squares and open diamonds, respectively.

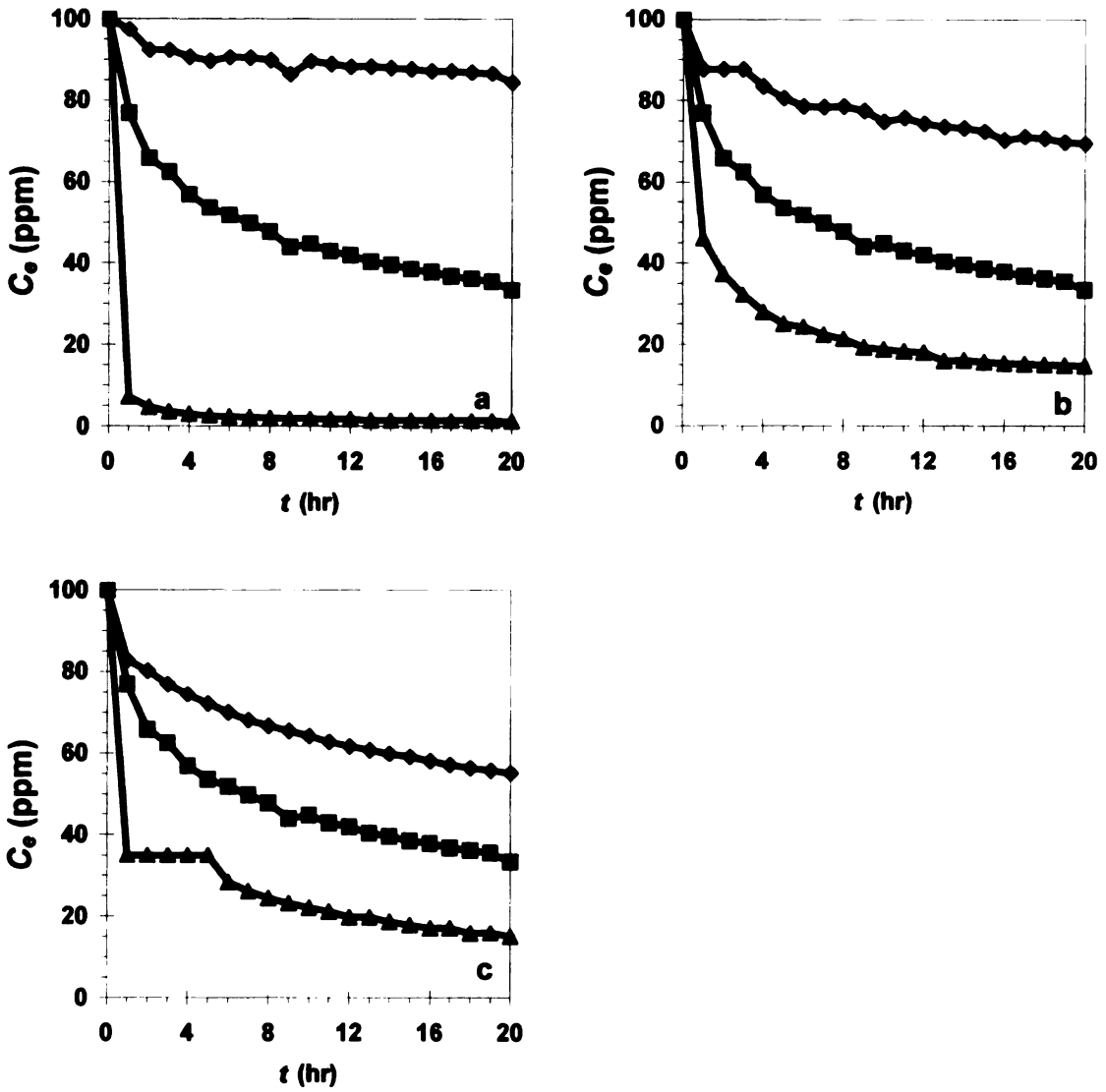

Figure 1-6. Extraction zone solute concentration histories obtained for variation of key parameters. (a) Three-well system with Q_e = 2.0 m^3/hr and k = 0.20 (diamonds), 2.0 (squares), and 20. hr^{-1} (triangles); (b) Two-well (diamonds), three-well (squares) and five-well (triangles) systems with Q_e = 2.0 m^3/hr and k = 2.0 hr^{-1}; (c) Three-well system with k = 2.0 hr^{-1} and Q_e = 8.0 (diamonds), 2.0 (squares) and 0.50 m^3/hr (triangles).

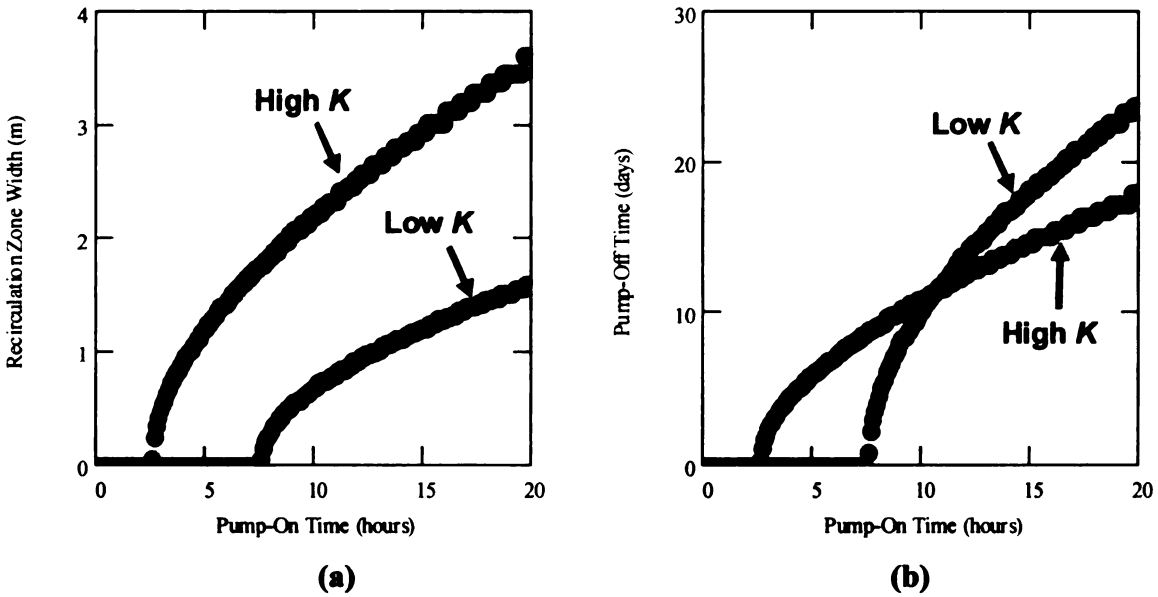

Figure 1-7. (a) Effective recirculation zone width and (b) maximum allowable pump-off time as a function of pump-on time for trap-and-treat operation in a confined two-layer heterogeneous aquifer. The conductivities of the low- and high-conductivity layers are 0.075 and 0.15 m/hr, respectively.

CHAPTER 2

Pulsed Pumping Process Optimization Using a Potential Flow Model

Nomenclature

a	spatial coordinate of point source/sink	(m)
B	maximum possible recirculation zone volume	(m^3)
E	exit-age residence time distribution	(hr^{-1})
F	feed-normalized residence time distribution	(-)
H	aquifer layer thickness	(m)
K	hydraulic conductivity	(m/hr)
L	well line length	(m)
M	number of aquifer layers	(-)
N	number of wells	(-)
P	aquifer porosity	(-)
Q	total pumping rate	(m^3/hr)
R	retardation factor for equilibrium linear sorption	(-)
S	well line stagger (offset)	(m)
t	pump-on time	(hr)
T	pump-off time	(hr)
v	fluid velocity	(m/hr)
V	natural gradient specific discharge	(m/hr)
w	complex potential function	(m^2/hr)
x	spatial coordinate perpendicular to natural gradient	(m)

y	spatial coordinate in the direction of natural gradient	(m)
z	complex spatial coordinate	(m)

Subscripts

j	layer index
k	well index
m	midpoint of timestep
max	layer with highest conductivity
min	layer with lowest conductivity

Introduction

Pulsed pumping or trap-and-treat remediation refers to the use of periodic rather than continuous pumping for capture and degradation of groundwater pollutants. In the pulsed system considered here, during the pump-off period, contaminants are transported by natural gradient groundwater flow into the region of the aquifer surrounding a transect of alternating injection and extraction wells. After a specified period of time has elapsed to permit intrusion of contaminated groundwater into this region, the well pumps are activated and a recirculation zone is established between adjacent injection and extraction wells along the well line. The extracted groundwater can be disposed of or treated for removal of contaminants and the aquifer recharged with clean water that is free of contaminants. Alternatively, the extracted groundwater can be augmented with chemicals or nutrients that stimulate abiotic or biological degradation of pollutants and then reinjected into the recirculation zone for *in situ* contaminant removal. Once the recirculation zone has been cleansed of contaminant, the pumps are shut off, allowing the next volume of contaminated groundwater to enter into the treatment zone by natural gradient flow. The alternating pump-off and pump-on modes of operation are continued sequentially for the duration of the project.

Pulsed pumping has been investigated, with varying levels of success, as a lower cost alternative to continuous pumping for the treatment of LNAPLs (Kim and Lee, 2002; Voudrias and Yeh, 1994), DNAPLs (Gerhard *et al.*, 1998; Whelan *et al.*, 1994) and VOCs (Mackay *et al.*, 2000). A hybrid scheme involving bioaugmentation and pulsed pumping has been developed for the *in situ* bioremediation of Schoolcraft Plume A, a carbon tetrachloride plume in near a village in southwest Michigan (Dybas *et al.*, 1998).

Bioaugmentation of Plume A with *Pseudomonas stutzeri* strain KC, a non-native microorganism, enabled transformation of more than 98% of the carbon tetrachloride in the groundwater into carbon dioxide and formate without production of chloroform over a 640-day monitoring period (Criddle *et al*, 1990; Dybas *et al.*, 1995; Dybas *et al.*, 2002). Pulsed pumping was implemented for the fifteen-well transect at the Plume A site, with a weekly five to ten hour pumping event for nutrient addition interrupting the slow (one meter per week) passage of the carbon tetrachloride-contaminated groundwater through the treatment zone and stimulating biodegradation of the chlorinated solvent by strain KC colonies in the aquifer solids. A substantial reduction of operating costs were realized in comparison to the projected expense for continuous pump-and-treat remediation of this site, which would have otherwise required pumping and disposal of large volumes of contaminated groundwater.

To achieve maximum effectiveness from the use of pulsed pumping in *in situ* remediation, the placement of injection/extraction wells and the pumping schedule must be sensibly chosen. Various mathematical models, based upon finite difference (Borden and Kao, 1992; Gerhard *et al.*, 2001), finite element (Armstrong *et al.*, 1994; Schulenberg and Reeves, 2002), Green's function (Harvey *et al.*, 1994) and boundary element (Zhang *et al.*, 1999) methods, have been put forth to evaluate pulsed pumping performance and economy relative to continuous pumping. Recently, a reactor model was developed for use as a computationally efficient pulsed pumping design and modeling tool (Tenney *et al.*, submitted). This reactor model is semi-analytic and thus resource efficient in comparison to MODFLOW (McDonald and Harbaugh, 1983) and MT3D (Zheng, 1992) numerical simulation methods. Comparison of the reactor model with finite difference

simulations has established that the model accurately predicts solute transport in systems with first-order reaction, fully-screened wells, and laterally homogeneous layers when dispersion is not large. The reactor model predictions also compare reasonably well with tracer breakthrough measurements from field experiments conducted at the Schoolcraft Plume A site. The semi-analytic reactor model is computationally efficient for optimization of the well configuration and groundwater extraction rate for pulsed pumping, and the effects of well density and pumping rate on degradation efficiency and operating costs were considered for several treatment grids (Tenney *et al.*, submitted). An interesting finding of this work is that there is an optimum intermediate value of the extraction rate, dependent on the number and configuration of wells, that maximizes contaminant degradation per unit of pumped groundwater volume. Preliminary calculations also suggested that an optimum schedule for pulsed pumping can be determined from the well geometry and aquifer hydrological profile. In this paper, we expand upon this latter concept and describe how potential flow and particle tracking algorithms can be combined into a predictive model for optimization of pumping schedules for pulsed pumping remediation systems.

Methodology

The aquifer is divided into laterally homogeneous layers with different values of natural gradient specific discharge V (Figure 2-1). N evenly spaced and fully screened injection/extraction wells are arranged in a line of length L perpendicular to the direction of natural gradient flow with the injection wells placed up- or downstream of extraction wells by a stagger distance S. (For the results described later in this study, S is uniformly set to zero.) During the pump-on periods, recirculation zones are established in each layer between adjacent injection and extraction wells (Figure 2-2). A recirculation zone is formally defined as the region between adjacent wells through which pumped water flows from the injection well to the extraction well. Because vertical flow is neglected, the recirculation zones in any given layer evolve independently of those in other layers.

The boundaries of a recirculation zone within a given layer depend upon the number of wells and their spacing and the dimensionless total pumping rate $Q^*=Q/(VHL)$, where Q is the total rate of groundwater extraction and H is the layer thickness. As the pumping rate or well spacing increases, the maximum possible volume of the recirculation zone likewise increases. Figure 2-2 shows the two-dimensional flow streamlines and resulting recirculation zones for any layer of a five-well system with $Q^*=30$ assuming an equal distribution of flow among injection and extraction wells. In a multi-layer system the value of Q^* is the same for all layers, eliminating the need to perform flow calculations for each layer.

The boundaries and volume of the recirculation zone are determined from an analytic potential flow model (Bird *et al.*, 1960; Columbini, 1999) that assumes steady-state, continuous, incompressible, inviscid, irrotational, two-dimensional flow occurs

within the layers of a confined aquifer. All injection and extraction wells are respectively assumed to be ideal sources and sinks. A solution for the flow field may be obtained in terms of the complex potential $w(z)$, where $z = x + iy$ and the natural groundwater gradient is in the positive direction of the y spatial coordinate. For an N-well system in an M-layer heterogeneous aquifer with even-numbered extraction wells staggered behind odd-numbered injection wells, the dimensionless complex potential $w^* = w_j/(LV_j)$ is

$$w^*(z^*) = \left[\sum_{k=1}^{N} \frac{Q_k{}^*}{2\pi} \ln(z^* - a_k{}^*)\right] + iz^* \tag{1}$$

$$Q_k{}^* = \begin{cases} \dfrac{Q^*}{\text{int}[(N+1)/2]}, & k \text{ odd} \\ -\dfrac{Q^*}{\text{int}[N/2]}, & k \text{ even} \end{cases} \tag{2}$$

$$a_k{}^* = \begin{cases} \left(-\dfrac{1}{2} + \dfrac{k-1}{N-1}\right) + i\dfrac{S^*}{2}, & k \text{ odd} \\ \left(-\dfrac{1}{2} + \dfrac{k-1}{N-1}\right) - i\dfrac{S^*}{2}, & k \text{ even} \end{cases} \tag{3}$$

$$Q^* = \frac{Q}{L\sum_{j=1}^{M} V_j H_j} \tag{4}$$

where int[x] is the truncated integer value of x, $z^* = z/L$, $S^* = S/L$, and H_j and V_j are the respective thickness and specific discharge of the jth layer. Equation (2) states that the total dimensionless pumping rate Q^* is distributed equally across the extraction wells and injection wells; e.g. for a three-well system with $S^* = 1$, groundwater is extracted at the rate $-Q^*$ from well 2 at coordinate $a_2^* = (0, -i/2)$, and injected at the rate $+Q^*/2$ into wells 1 and 3 at coordinates $a_1^* = (-1/2, +i/2)$ and $a_3^* = (+1/2, +i/2)$.

The velocity field $v_j(z)$ of layer j may be obtained from the derivative of the complex potential

$$v_j(z) = \frac{dw_j}{dz} = V_j \left\{ \left[\sum_{k=1}^{N} \frac{Q_k^*}{2\pi} \frac{1}{(z^* - a_k^*)} \right] + \mathrm{i} \right\} \tag{5}$$

where the velocity components v_x and v_y are given respectively as the real and imaginary parts of equation (5).

As previously noted, pulsed pumping is characterized by long periods where the remediation system is idle, punctuated by recurrent pumping events in which the contaminated groundwater that has entered the treatment zone is purged and replaced with clean or augmented water. An estimate of the allowable pump-off time for the trapping phase, as a function of the pump-on time for the treatment phase, can be obtained if the recirculation zone residence time distribution $E(t)$ is known for each pair of adjacent wells in an aquifer layer. Assuming that contaminated groundwater is continuously extracted during the pump-on phase and replaced by clean injected water, the fraction of a recirculation zone volume that is fully swept by the injected water is equal to the value of the feed-normalized residence time distribution $F(t)$. For pumping time t

$$F(t) = \int_0^t E(\tau)\mathrm{d}\tau \,. \tag{6}$$

For each recirculation zone $E(\tau)$ is calculated using a second-order numerical particle-tracking algorithm in which a predetermined number of particles are uniformly distributed around the circumference of the injection well. Using the flow field solution obtained from equation (1), the trajectory of each particle is tracked forward in time until it either reaches an extraction well or it moves a specified distance from its original

position (i.e. along a streamline directed outside of the recirculation zone). The latter particles are discarded from the analysis of the recirculation zone residence time distribution. The location of a particle at the end of the next timestep is calculated from its current position and from the velocity field of equation (5) as

$$z^*(t + \Delta t) = z^*(t) + [\ v_m^* / |v_m^*|\ ]\ \Delta t \tag{7}$$

$$v_m^* = v^*(\ z^* + \tfrac{1}{2}\ [\ v^*(z^*) / |v^*(z^*)|\ ]\ \Delta t) \tag{8}$$

where Δt is the time increment and the dimensionless velocity $v^*(z^*) = -v_x/V + iv_y/V$ at the dimensionless spatial coordinate z^*.

Once the residence time distribution has been numerically determined, $F(t)$ is calculated by discretizing the integral of equation (6). The product of $F(t)$ and the maximum possible recirculation zone volume B is equivalent to the volume traversed by those streamlines in the recirculation zone that arrive at the extraction well within the pumping interval t. Dividing the volume of this swept zone by the well spacing, $L/(N-1)$, and the aquifer layer thickness yields an estimate of the swept recirculation zone width. In the absence of significant degradation or sorption, the allowable pump-off time $T_j(t)$ for a given layer for pump-on time t is the time required for a parcel of groundwater traveling at the natural gradient groundwater flow velocity to cross the swept width of the narrowest recirculation zone in this layer during the idle period of no pumping activity:

$$T_j(t) = (N-1)BF(t)/(LH_jV_j) \tag{9}$$

In this manner, permissible pump-off times (i.e. those which avoid contaminant breakthrough) can be estimated for separate layers in a heterogeneous aquifer, given a specified well geometry, the aquifer physical properties, and the duration and rate of groundwater extraction maintained during the pump-on period. A presentation of results

and observations using this method for a broad range of model aquifer/well systems now follows.

Results

Figure 2-3 shows the maximum pump-off time as a function of pump-on time for an arbitrary pulsed pumping system operating in a three layer heterogeneous aquifer consisting of a low, medium, and high conductivity (K) layer. While all aquifer layers in the system have the same maximum possible steady state recirculation zone width, during pulsed pumping operation the swept recirculation zone width increases most rapidly with pump-on time for the highest conductivity layer, and least rapidly for the lowest conductivity layer. This is reflected in the shapes of the pump-off time vs. pump-on time curves $Tj(t)$ shown for the three layers in Figure 2-3. If the pulsed pumping timetable is constrained so as to avoid breakthrough of contaminated water in all layers, then the maximum allowable pump-off time for any given pump-on interval t is given by the minimum of the T_1, T_2 and T_3 curves at that value of t. This maximum pump-off time to prevent breakthrough in any layer is depicted by the solid line in Figure 2-3.

It can be seen that for pump-on intervals of less than 13.6 hours, the allowable pump-off time is constrained by the breakthrough of contaminant in the lowest conductivity layer. The reason for this is that the swept width of the recirculation zone in this layer is narrower than in the higher conductivity layers. In fact, it is apparent from Figure 2-3 that, in order for pulsed pumping to be carried out in this model aquifer, the pumps must remain activated for at least twelve hours during each pump-on interval. For pumping durations shorter than this, there is insufficient time to fully sweep the recirculation zone of the lowest conductivity layer; i.e. none of the water injected into this layer reaches the extraction well within the allotted time period, reducing the allowable pump-off zero.

Conversely, for pumping durations that exceed 13.6 hours, the allowable pump-off time becomes constrained by the highest conductivity layer. Although the swept width of the recirculation zone is always larger in this layer than in the other layers, natural gradient flow is also fastest in the highest conductivity layer, and so it takes less time for a parcel of groundwater to cross the swept width of this layer compared with the other layers. The crossover point, at which the most and least conductive aquifer layers have the same breakthrough time, occurs for the pump-on interval of 13.6 hours for the particular model aquifer considered in Figure 2-3. Significantly, the fractional pump-on time for pulsed pumping passes through a minimum at this pumping duration. Maximum operational efficiency is achieved by adopting the pumping schedule corresponding to the crossover point; i.e. activating the pumps for 13.6 hours, and then idling the pumps for 2.2 days. Pump-on times shorter than 13.6 hours are disadvantageous because rapid breakthrough in the swept zone of the lowest conductivity layer compels more frequent pumping. Pump-on times longer than the optimum are also disadvantageous because the potential benefit of a longer pump-off time interval is negated by an overall increase in the fraction of time that the pumps are turned on. Departures from the pumping schedule at the crossover point in either direction therefore lead to increased operating costs due to the energy expended in groundwater extraction and re-injection.

For well configurations or aquifer constructs that have different physical properties than those considered in Figure 2-3, the preceding analysis will naturally yield a different optimum pumping schedule. However, the same process optimization considerations will apply. It is noteworthy that the properties of the aquifer layer with

intermediate conductivity had no bearing on the determination of the process optimum in Figure 2-3; i.e. only the conditions in the highest and lowest conductivity layers were significant to the outcome. It can be shown that for multi-layered, heterogeneous systems, the minimum fraction of pump-on time will always occur where allowable pump-off times for the least and most conductive layers become equal. (For single-layer systems the minimum required fraction of pump-on time occurs when the slope of allowable pump-off time versus pump-on time, dT/dt, is equal to T/t.) Consequently, finding the optimal pumping scheme for pulsed pumping in an aquifer that has three or more physically distinct vertical layers simplifies to an analysis of contaminant breakthrough in just two of the layers, those that have the highest and the lowest specific discharge, and the pump-on vs. pump-off correlations may be expressed in terms of a specific discharge ratio $V^* = V_{max}/V_{min}$ for the most conductive and least conductive layers.

Discussion

Figure 2-4 is a plot of dimensionless pump-off time versus dimensionless pump-on time for a single layer with all combinations of N = 5, 7, 9, 11, 13, 15, 21, 31, 45, 67, and 99 wells and dimensionless total pumping rates $Q^* = Q/(VHL)$ = 12, 20, 30, 50, 80, 120, 200, and 300. Pump-off time is shown in units of $PRL/[V(N\text{-}1)]$ where P is aquifer porosity and R is a retardation factor accounting for sorption effects. A dimensionless pump-off time T^* equal to unity corresponds to the time required to cross a recirculation zone with a width equal to the well spacing, i.e. T^* could equivalently be referred to as the recirculation zone width in units of $L/(N\text{-}1)$. Pump-on time is shown in units of

$$\frac{PRL}{V(N-1)} \cdot \frac{\pi N}{6Q^*(N-1)} \cdot \frac{1}{1.948\exp(-0.694N)+0.0001081N+0.757} \tag{10}$$

The first two terms in (10) represent the time required to travel directly between any pair of adjacent (and unstaggered) injection and extraction wells in the absence of natural gradient flow and neglecting influences from other wells in the system. The third term in (10) is an empirical correction to account for the influence of other wells in the system upon the travel time between the adjacent wells. This empirical correction was used for presentation of the data instead of the exact expression because calculating exact inter-well travel times for systems with an arbitrary number of wells is very cumbersome. Presented in the units described above, a dimensionless pump-on time t^* equal to unity roughly corresponds to the initial breakthrough of recirculation flow between the adjacent wells. Substituting the definition of Q^* into (10), it can be seen that this breakthrough time is proportional to $[L/(N\text{-}1)]^2$, which is the square of the well separation distance, and inversely proportional to $Q/(2NH)$, which is roughly equal to the pumping rate per unit layer thickness per well.

Using least-squares regression, the data was fit to the equation

$$T^* = 0.5404(t^*-1)0.5292 - 0.0766(t^*-1) \quad (11)$$

Note that this equation is empirical and should not be extrapolated beyond its maximum value at approximately $t^*=17$. As shown in Figure 2-4 by the curve of $t^*/(t^*+ T^*)$, the required fraction of pump-on time for a single-layer system reaches a minimum value when the dimensionless pump-on time is approximately equal to 1.85. The dimensionless pump-off time at that point is approximately 0.44, which corresponds to a recirculation zone width equal to 44% of the distance between adjacent wells. Actual fractions of time spent with pumps on may be calculated from $t^*/(t^*+T^*)$ and the definitions of t^* and T^*.

Although not shown in Figure 2-4, systems with three wells generally have longer allowable pump-off times than systems with more wells because only in three-well systems are all recirculation zones the same size and shape. Three well systems are particularly efficient because the narrowest recirculation zone in a layer determines the maximum pump-off time and remaining recirculation zones might be considerably wider. As stated earlier, total extraction and injection rates were assumed to be distributed equally among extraction and injection wells, respectively. With an odd number of wells greater than three under these pumping conditions, the recirculation zone between the second and third well is always the narrowest. For systems with Q^* greater than 10, the width of this recirculation zone approaches a limiting value approximately equal to 110% of the distance between adjacent wells. Systems with Q^* less than 10 approach limiting recirculation zone values less than this distance and so generally have shorter allowable pump-off times. Cursory investigation suggests that overall pumping requirements for

pulsed operation could be reduced if individual well pumping rates were adjusted to result in a more even distribution of recirculation flow between various well pairs. For example, the calculated pumping requirements for a single layer, 15-well system operating at Q^*=30 were reduced by approximately 12% by simply adjusting flow rates to result in the same fluid velocity at the midpoints of the gaps between all pairs of adjacent wells. Further study is required to determine whether this strategy would be beneficial in a field setting.

If it is necessary to account for degradation or non-linear sorption during the pump-off period, this more complicated behavior can be simulated by combining equation (11) with a customized one-dimensional flow model. In this case equation (11) is used to calculate the recirculation zone width, and the one-dimensional flow model is used to calculate the allowable pump-off time by simulating contaminant transport across the recirculation zone width. A similar adjustment could also be made to the pump-on time if necessary, but it would be less straightforward because the effect would need to be spread over a continuum of path lengths, which are not explicitly shown in equation (11).

Although equation (11) applies specifically to recirculation zone behavior in only one layer, it can be used to predict the behavior of multi-layer systems. Recalling that $V^*=V_{max}/V_{min}$, if $T^*=f(t^*)$ is the allowable pump-off time for the layer with the greatest superficial velocity, then $V^*f(t^*/V^*)$ is the allowable pump-off time for the layer with the lowest superficial velocity. The allowable pump-off time for the entire system at any given value of t^* is then the minimum of the two values $f(t^*)$ and $V^*f(t^*/V)$. Note that in this case the superficial velocity used to convert the actual pump-off and pump-on times from their dimensionless forms is V_{max}. Also note that the allowable pump-off time for

layers with intermediate values of conductivity can be similarly calculated but that these layers have no influence on the allowable pump-off time for the entire system.

Predictions made by equation (11) were compared to published results (Hyndman *et al.*, 2000) describing an optimization study conducted using the MODFLOW finite difference groundwater flow model to design a pulsed-pumping system intended to feed microbes once per week in a 15m deep x 15m long x 0.3m wide bioremediation zone. (Based upon the published aquifer characteristics, V=0.356 m/week, P=0.3, and R=1 were chosen to calculate t from (10) and equation (11) for various N and Q.) Figure 2-5 summarizes the results of this comparison by plotting the predicted total pumped volume per pumping event versus number of wells for 7-, 9-, 11-, 13-, and 15-well systems. (Total pumped volumes from Hyndman were calculated from values apparently published on a per-well basis.) The agreement between the predictions from equation (11) and the MODFLOW simulations is very good. As is commonly the case, significant information about aquifer heterogeneity was not available prior to installing the remediation system in question, and so initial design simulations had to be conducted using relatively simple aquifer models. This necessarily simplified approach was continually validated as more data became available (Hyndman *et al.*, 2000). Note that equation (11) inherently assumes that the total pumped volume per pumping event remains constant regardless of the actual pumping rate chosen if the final recirculation zone width is specified. This is equivalent to stating that pump-on time varies inversely with pumping rate for a given number of wells. In support of this assumption, it was found using conventional groundwater models to simulate the system described above

that total pumped volumes varied by less than 3% while varying total pumping rates from 0.4 to 125 m^3/hr (Hyndman *et al.*, 2000).

The pulsed-pumping schedule (i.e. pump-on and pump-off time) that minimizes total pumped volume for an N-well system operated at dimensionless total pumping rate Q^* and installed in a heterogeneous aquifer with superficial velocity ratio V^* was identified for all combinations of N = 3, 5, 7, 9, 11, 13, 15, 21, 31, 45, 67, 99; Q^* = 2, 3, 5, 8, 12, 20, 30, 50, 80, 120, 200, 300; and V^* = 1, 2, 3, 5, 8, 12, 20, 30, 40. Results from these calculations are presented in Figures 6-9.

Figure 2-6 is a plot of the dimensionless pump-on time t^* for most efficient pumping versus the superficial velocity ratio for 7- to 99-well systems operating at various dimensionless total pumping rates. Calculations for systems with three or five wells generally yield larger values of t^*. The pump-on time for multi-layer systems is shown in units of

$$V^* \cdot \frac{PRL}{V_{\max}(N-1)} \cdot \frac{\pi N}{6Q^*(N-1)} \cdot \frac{1}{1.948\exp(-0.694N)+0.0001081N+0.757} \qquad (12)$$

which reduces to (10) for single-layer systems. As previously seen in Figure 2-4, t^* approaches a value of approximately 1.85 for homogeneous aquifers, i.e. when V^*=1. Also note that the dimensionless pump-on time for any given Q^* decreases to a limiting value as V^* increases. The value of V^* at which t^* becomes constant is equal to the value of t^* at which the recirculation zone width reaches its maximum limiting value in the most conductive layer for that pumping rate. Although the dimensionless pump-on time for most efficient pumping decreases with increasing V^*, the actual pump-on time t must always increase with V^*.

Figure 2-7 is a plot of the dimensionless pump-off time T^* for most efficient pumping versus the dimensionless total pumping rate for 7- to 99-well systems in aquifers with various degrees of layered heterogeneity, as measured by V^*. Calculations for systems with three or five wells generally yield larger values of T^*. As expected, pump-off times approach zero as Q^* approaches unity, and continuous pumping becomes necessary when pumping is no longer strong enough to establish recirculation zones between all wells. Figure 2-7 also shows that the most efficient pump-off time does not change significantly as Q^* is increased beyond a particular value for any given V^*. Similarly, pump-off time does not change significantly as V^* is increased beyond approximately 12 for any given pumping rate. The combination of V^* and Q^* values above which T^* becomes constant is again related to the point at which the recirculation zone width reaches its maximum limiting value in the most conductive layer.

Figure 2-8 is a plot of the minimum possible fraction of time spent with pumps turned on versus dimensionless total pumping rate for 3- to 99-well systems in aquifers with various degrees of layered heterogeneity. Figure 2-8 provides a quantitative estimate of how required system operation varies from continuous pumping through degrees of pulsed pumping as the total pumping rate is changed. Figure 2-8 also shows that heterogeneity can have a significant negative impact upon overall pumping requirements. As seen previously in Figure 2-7, pumping becomes continuous as Q^* approaches unity and recirculation between wells becomes nonexistent. Because Figure 2-8 assumes retardation and degradation are negligible, for pulsed operation the actual required fraction of time spent with pumps on will be lower than that shown in Figure 2-8

if retardation and/or degradation are significant due to the increase in allowable pump-off time.

Figure 2-9 is a plot of the minimum possible time-averaged dimensionless total pumping rate versus dimensionless total pumping rate for 3- to 99-well systems in aquifers with various degrees of layered heterogeneity. The average total pumping rate is calculated by multiplying the fraction of time spent with pumps on (from Figure 2-8) by the total pumping rate. Figure 2-9 provides a quantitative estimate of the degree of retardation and/or degradation required in order to provide pulsed-pumping with an efficiency advantage relative to continuous pumping. For example, if retardation and degradation are negligible during the pump-off phase (as is assumed in Figures 8 and 9), pulsed operation will always increase pumping requirements relative to continuous operation. This potential disadvantage for pulsed systems relative to continuous systems becomes more significant as heterogeneity increases. Because this model assumes only two-dimensional flow, actual flow through low conductivity layers might be reduced relative to model predictions for systems in which significant vertical flow between layers is possible. This would result in an effective value of V^* greater than the calculated value of V^*, worsening the case for pulsed operation.

Conclusion

The two-dimensional potential flow model and recirculation zone analysis presented in this work is intended as a tool for initial design of *in situ* remediation systems that employ pulsed pumping. The model provided predictions comparable to those from a conventional finite-difference groundwater flow model used during the initial design and cost-analysis of a pulse pumped bioremediation system. A virtue of the semi-analytic model is its speed of application for identifying the pulsed pumping schedule best-suited for a given well configuration and aquifer physical properties. For selection of the pumping schedule, the principal constraint applied is that pumping costs are to be minimized by selecting the largest possible ratio of pump-off time to total pumped groundwater volume, subject to the requirement that contaminant breakthrough in the swept portion of the recirculation zone during the pump-off period is prohibited. Bioremediation systems may be additionally constrained by the feed requirements of the *in situ* microbial population, and may therefore necessitate pulsed pumping of enriched nutrient medium more frequently than would otherwise be adopted based on hydrologic considerations alone.

The results from this model provide a lower bound to pulsed pumping requirements, particularly for systems with a high degree of vertical heterogeneity. The model predictions are based upon hydrologic considerations and do not take into account dispersion or vertical flow in the recirculation zone during the pump-on phase, which may be significant in some aquifers. If the actual system uses partially-screened wells, flow paths making up the upper and lower regions of the recirculation zone will tend to be longer than predicted by this model. Similarly, since some degree of vertical flow

between layers of differing conductivity will likely be present during pumping events, actual flow through the recirculation zone of low conductivity layers will likely be reduced relative to that predicted by this model, and so a greater amount of pumping will be required. In such cases, three-dimensional groundwater flow models are recommended for carrying out final process optimization; or alternatively, a scale factor for the recirculation zone RTD can be applied to mimic for the longer fluid streamlines in three-dimensional flow.

Figures

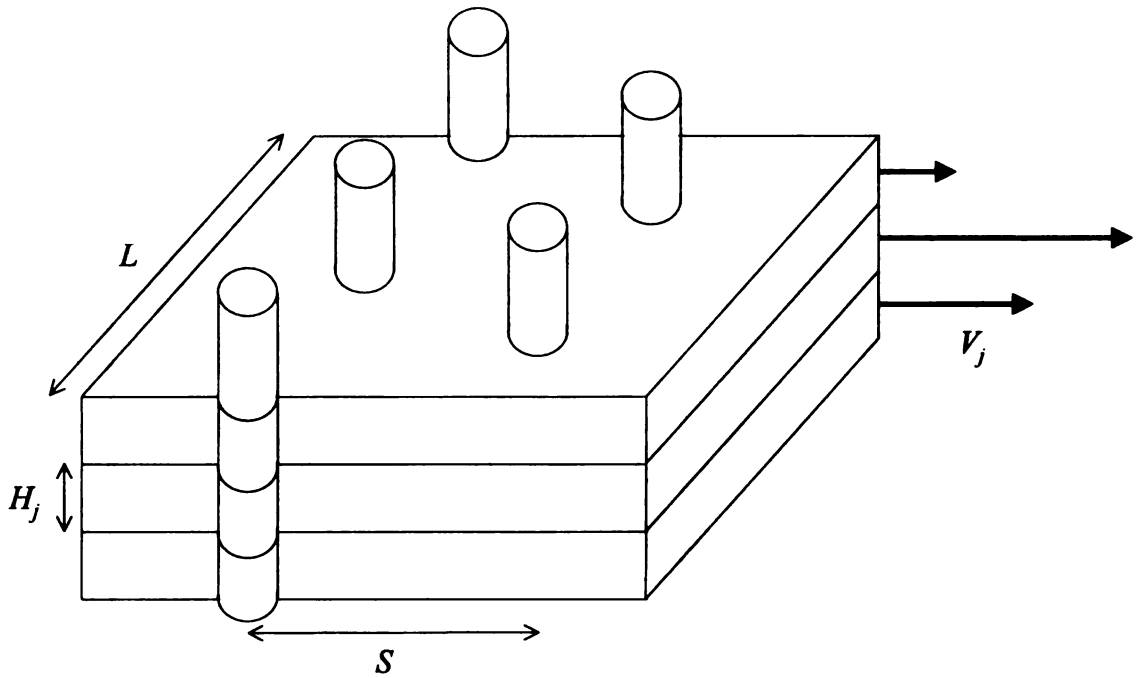

Figure 2-1. Model aquifer structure and well geometry used for analysis of pulsed pumping. The geometric parameters for well length, well stagger, and aquifer layer thickness are shown for a hypothetical five-well, three-layer system with vertical heterogeneity, as indicated by the layer-dependent specific discharge.

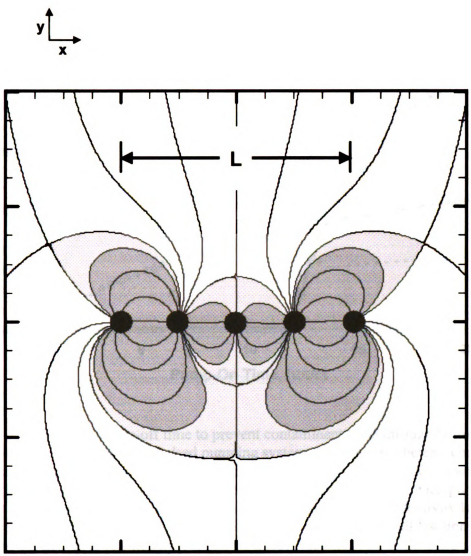

Figure 2-2. Streamlines obtained from potential flow model for an unstaggered, five-well system in a single confined aquifer layer with $Q^*=Q/(VHL)=30$ and an equal distribution of flow between all injection and extraction wells. If natural gradient groundwater flow is assumed to be in the positive y-direction, three wells are extracting groundwater and two wells are injecting. The recirculation zone is highlighted.

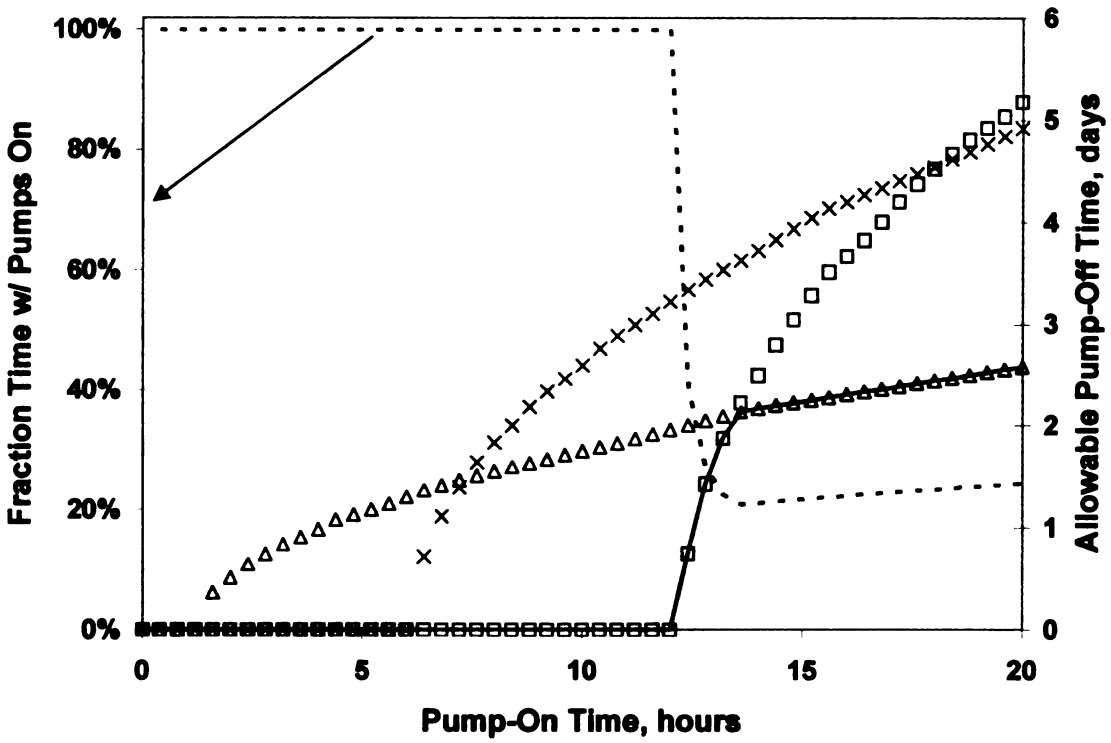

Figure 2-3. Allowable pump-off time to prevent contaminant breakthrough between pumping events for an arbitrary pulsed pumping system operating in a heterogeneous aquifer consisting of a low, medium, and high conductivity (*K*) layer. The allowable pump-off time is shown on the right axis as a function of the duration of each pumping event for the low (squares), intermediate (x's) and high (triangles) conductivity layers considered separately, and for the entire aquifer (solid line). The overall fraction of time the pumps are activated (dashed line) is shown on the left axis.

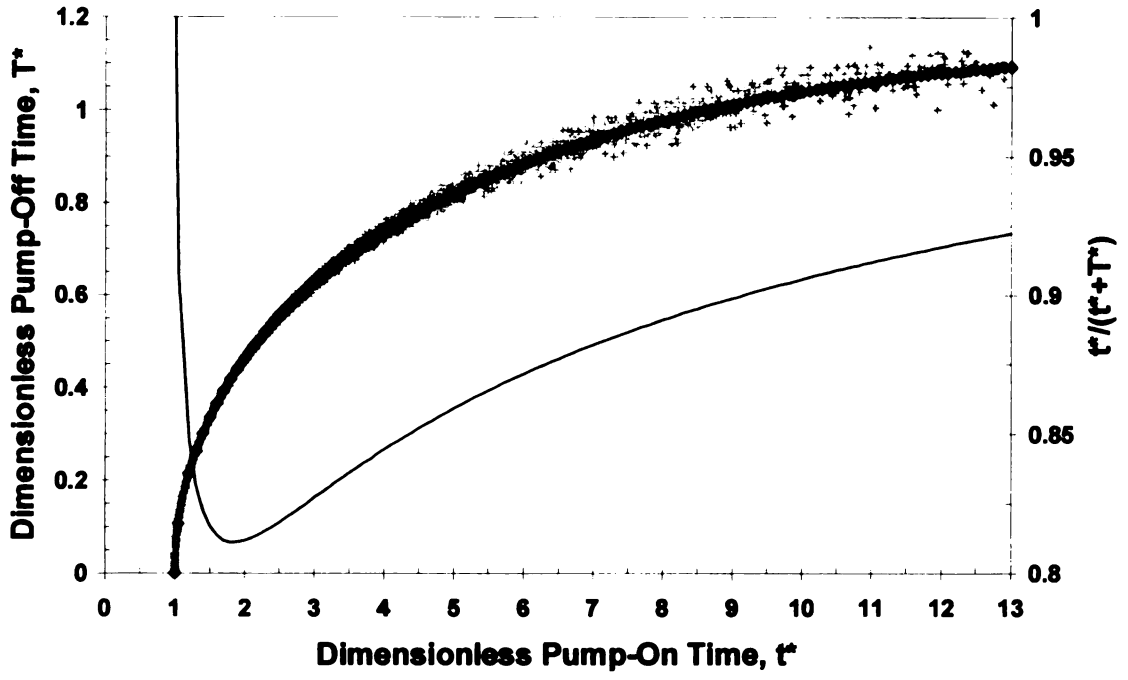

Figure 2-4. Dimensionless allowable pump-off time T^* versus dimensionless pump-on time t^* for single-layer systems. All combinations of N = 5, 7, 9, 11, 13, 15, 21, 31, 45, 67, 99 wells and dimensionless total pumping rates $Q^* = Q/(VHL)$ = 12, 20, 30, 50, 80, 120, 200, 300 are represented (scattered +'s). $T^*=T[V(N\text{-}1)/(PRL)]$. $t^*=t[V(N\text{-}1)/(PRL)][6Q^*(N\text{-}1)/(\pi N)][1.948\exp(-0.694N)+0.0001081N+0.757]$. Note that T^* could equivalently be referred to as the recirculation zone width in units of L/(N-1). The data were fit to the equation $T^*=f(t^*)=0.5404(t^*\text{-}1)0.5292\text{-}0.0766(t^*\text{-}1)$ via least-squares regression (solid diamonds). The minimum of the $t^*/(t^*+T^*)$ curve (solid line) corresponds to the point of operation for maximally efficient pumping. Actual fractions of time spent with pumps on may be calculated from $t^*/(t^*+T^*)$ and the definitions of t^* and T^*.

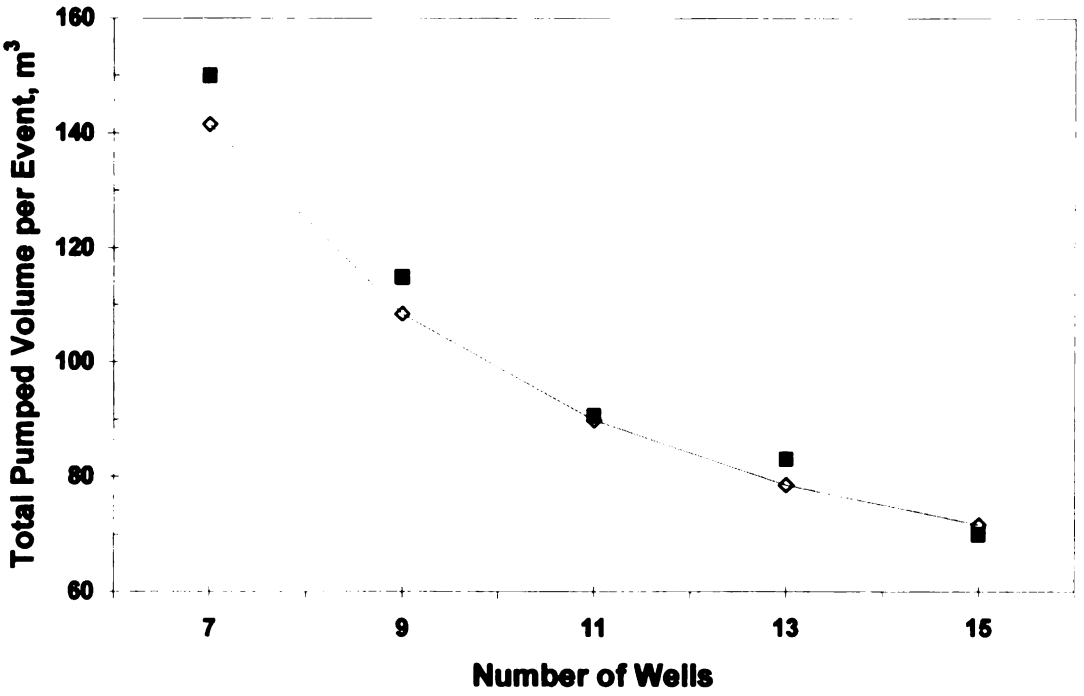

Figure 2-5. Total pumped volume required to flush a 15m deep x 15m long x 0.3m wide bioremediation zone versus the number of wells in the system. Values predicted by the potential flow model (connected diamonds) are compared with values calculated using a MODFLOW finite-difference groundwater flow model (solid squares, Hyndman et al. 2000). Values of V=0.356 m/week, P=0.3, and R=1 were applied to the potential flow model based upon the published aquifer characteristics.

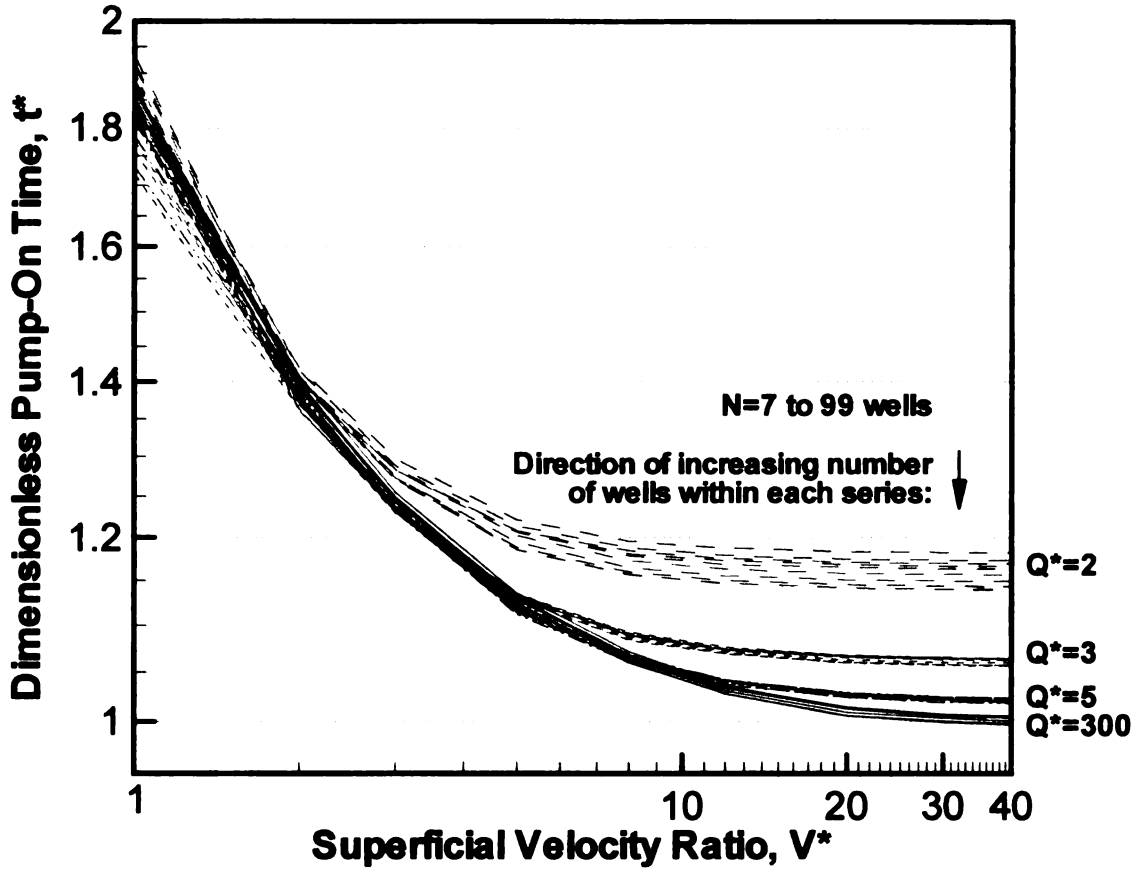

Figure 2-6. Pump-on times that minimize total pumping requirements for pulsed pumping systems operated in heterogeneous aquifers. Dimensionless pump-on time t* is plotted against the superficial velocity ratio $V^* = V_{max}/V_{min}$ for systems with various dimensionless total pumping rates $Q^*=Q/(VHL)$. Systems with $N = 7, 9, 11, 13, 15, 21, 31, 45, 67$, and 99 wells are represented. $t^*=t[1/V^*][V_{max}(N\text{-}1)/(PRL)][6Q^*(N\text{-}1)/(\pi N)][1.948\exp(-0.694N)+0.0001081N+0.757]$.

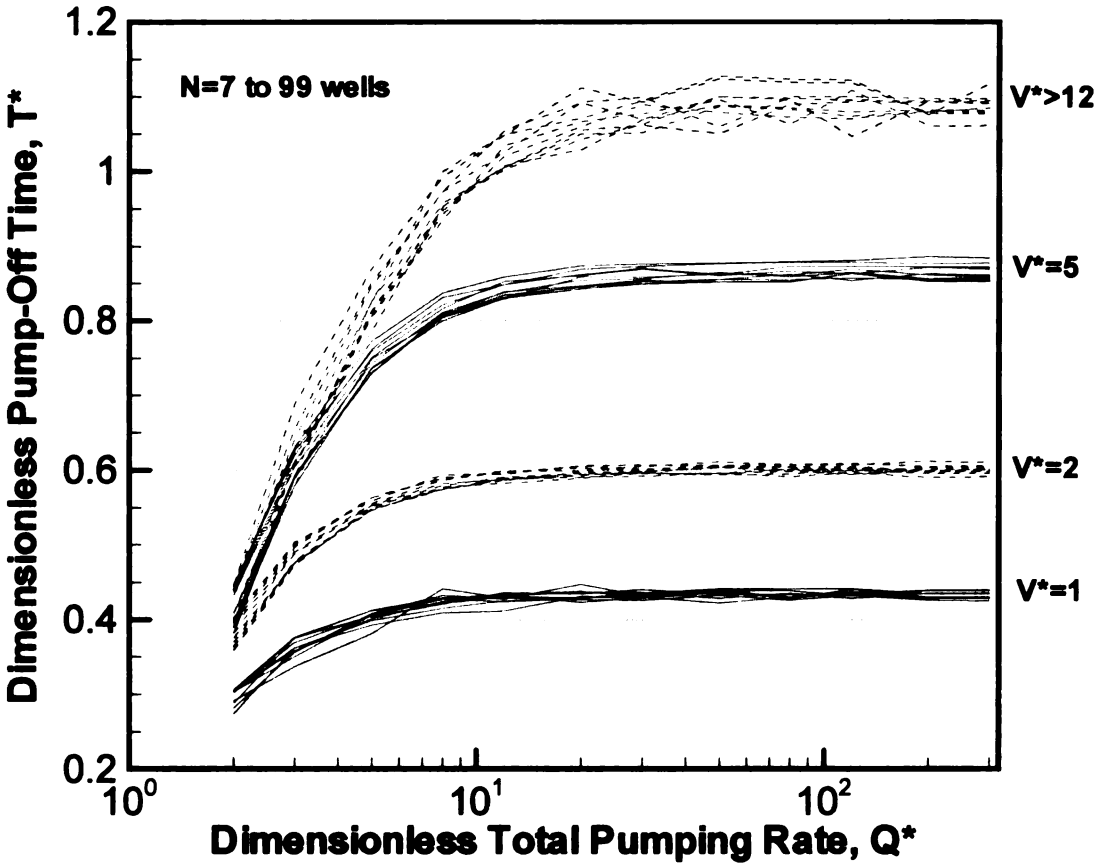

Figure 2-7. Pump-off times that minimize total pumping requirements for pulsed pumping systems operated in heterogeneous aquifers. Dimensionless pump-off time T^* is plotted against dimensionless total pumping rate Q^* for systems with various degrees of vertical heterogeneity, as measured by the superficial velocity ratio V^*. Systems with $N = 7, 9, 11, 13, 15, 21, 31, 45, 67$, and 99 wells are represented. $T^*=T[V(N\text{-}1)/(PRL)]$.

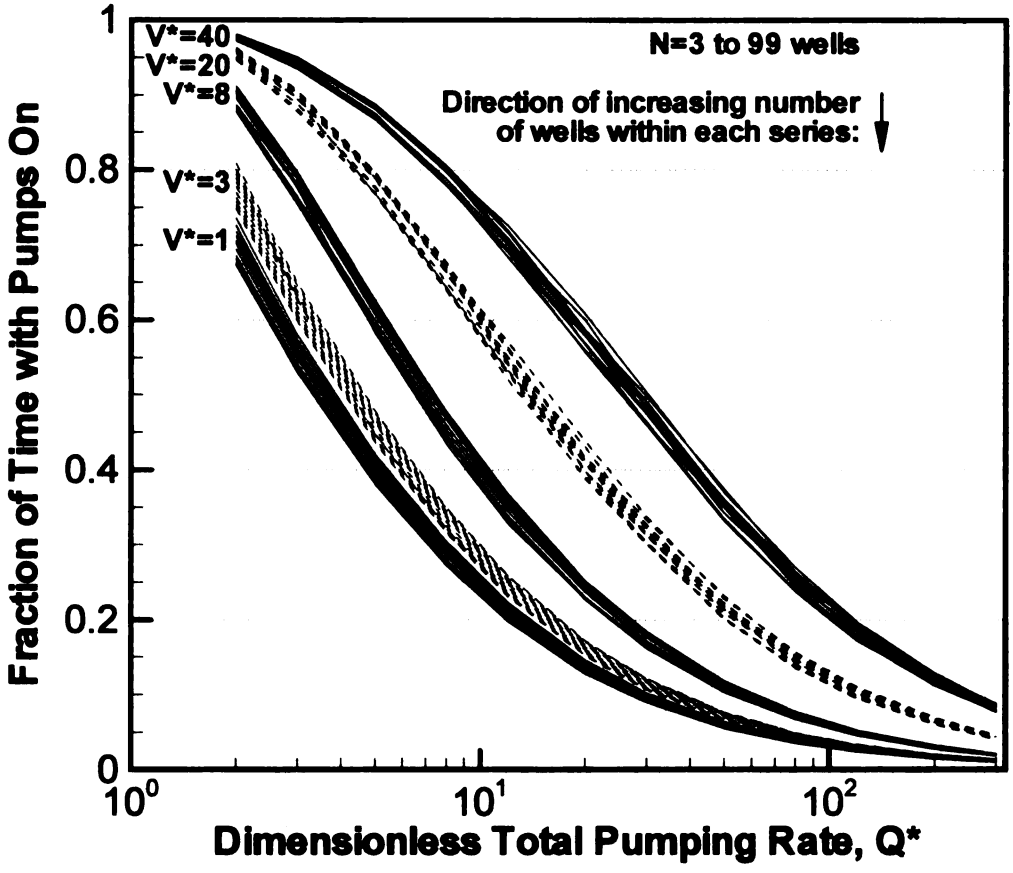

Figure 2-8. Minimum required fraction of time with pumps on for pulsed pumping systems operated in heterogeneous aquifers. The fraction of pump-on time resulting from use of the most efficient pulsed pumping schedule is plotted against dimensionless total pumping rate Q^* for systems with various degrees of vertical heterogeneity, as measured by the superficial velocity ratio V^*. Systems with $N = 3, 5, 7, 9, 11, 13, 15, 21, 31, 45, 67$, and 99 wells are represented.

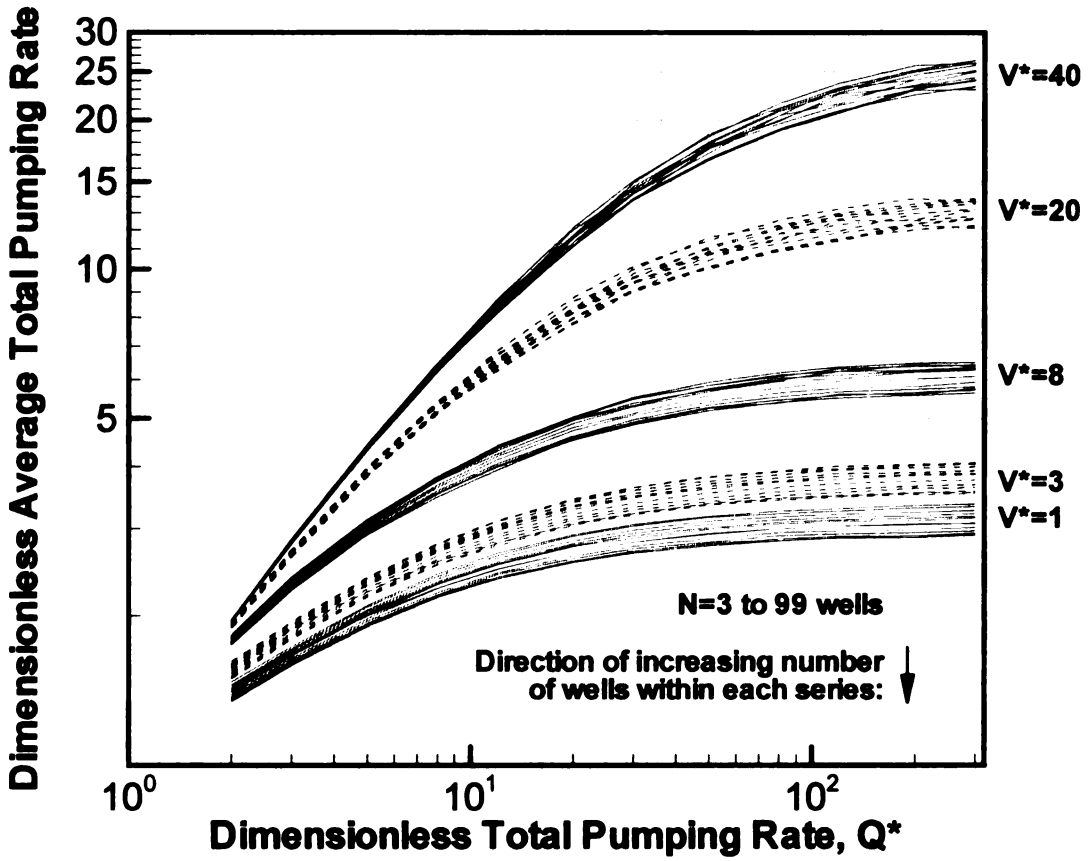

Figure 2-9. Minimum possible average dimensionless total pumping rate for pulsed pumping systems operated in heterogeneous aquifers. The average dimensionless total pumping rate resulting from use of the most efficient pulsed pumping schedule is plotted against dimensionless total pumping rate Q^* for systems with various degrees of vertical heterogeneity, as measured by the superficial velocity ratio V^*. Average total pumping rate is the product of the fraction of pump-on time and the total pumping rate. Systems with $N = 3, 5, 7, 9, 11, 13, 15, 21, 31, 45, 67$, and 99 wells are represented.

REFERENCES

Armstrong, J.E., Frind, E.O. and McClellan , R.D. (1994) Nonequilibrium mass-transfer between the vapor, aqueous, and solid-phases in unsaturated soils during vapor extraction. *Water Resources Research* **30**, 355-368.

Bakker, M. and Strack, O. (1996) Capture zone delineation in two-dimensional groundwater flow models. *Water Resources Research* **32**, 1309-1315.

Bird, R.B., Stewart, W.E. and Lightfoot, E. N. (1960) *Transport Phenomena*, pp. 134-135, John Wiley and Sons, New York, NY.

Borden, R.C. and Kao, C.M. (1992) Evaluation of groundwater extraction for remediation of petroleum-contaminated aquifers. *Water Environment Research* **64**, 28-36.

Columbini, M. "Irrotational Plane Flows of an Inviscid Fluid", http://www.diam.unige.it/~irro/.

Criddle, C. S., DeWitt, J.T., Grbic-Galic, D. and McCarty, P.L. (1990) Transformation of carbon tetrachloride by *Pseudomonas sp.* strain KC under denitrification conditions. *Applied and Environmental Microbiology* **56**, 3240-3246.

Dybas, M.J., Tatara, G.M. and Criddle, C. S. (1995) Localization and characterization of the carbon tetrachloride transformation activity of *pseudomonas sp.* strain KC. *Applied Environmental Microbiology* **61**, 758-762.

Dybas, M. J., Barcelona, M., Bezborodnikov, S., Davies, S., Forney, L., Heuer, H., Kawka, O., Mayotte, T., Sepúlveda-Torres, L., Smalla, K., Sneathen, M., Tiedje, J., Voice, T., Wiggert, D.C., Witt, M.E. and Criddle, C.S. (1998) Pilot-scale evaluation of bioaugmentation for *in situ* remediation of a carbon tetrachloride contaminated aquifer. *Environmental Science and Technology* **32**, 3598-3611.

Dybas, M.J., Hyndman, D.W., Heine, R., Tiedje, J., Linning, K., Wiggert, D., Voice, T., Zhao, X., Dybas, L., and Criddle, C.S. (2002) Development, operation, and long-term performance of a full-scale biocurtain utilizing bioaugmentation. *Environmental Science & Technology* **36**, 3635-3644.

Fogler, H.S. (1999) "Elements of Chemical Reaction Engineering" (3rd edition), pp. 838-844, Prentice Hall, Upper Saddle River, NJ.

Gerhard, J.I., Kueper, B.H. and Hecox, G.R. (1998) The influence of waterflood design on the recovery of mobile DNAPLs. *Ground Water* **36**, 283-292.

Gerhard, J.I., Kueper, B.H. Hecox, G.R. and Schwarz, E.J. (2001) Site-specific design for dual phase recovery and stabilization of pooled DNAPL. *Ground Water Monitoring and Remediation* **21**, 71-88.

Harvey, C.F., Haggerty, R. and Gorelick, S.M. (1994) Aquifer remediation: a method for estimating mass-transfer rate coefficients and an evaluation of pulsed pumping. *Water Resources Research* **30**, 1979-1991.

Hyndman, D.W., Dybas, M.J. and Forney, L.(2000) Hydraulic characterization and design of a full-scale biocurtain. *Ground Water* **38**, 462-474.

Kim, J.S. and Lee, K. (2002) Influence of alcohol cosurfactants on surfactant-enhanced flushing of diesel-contaminated soil. *Journal of Environmental Science and Health* **37**, 1051-1062.

Levenspiel, O. (1999) "Chemical Reaction Engineering" (3rd edition), pp. 101-112, John Wiley and Sons, New York, NY.

Mackay, D.M., Wilson, R.D., Brown, M.J., Ball, W.P., Xia, G. and Durfee, D.P. (2000) A controlled field evaluation of continuous vs. pulsed pump-and-treat remediation of a VOC-contaminated aquifer: site characterization, experimental setup, and overview of results. *Journal of Contaminant Hydrology* **41**, 81-131.

Mayotte, T.J., Dybas, M.J. and Criddle, C.S. (1996) Bench scale evaluation of bioaugmentation and transformation of carbon tetrachloride in a model aquifer system. *Groundwater* **34**, 358-367.

McDonald, M.G. and Harbaugh, A.W. (1988) A modular three-dimensional finite-difference ground-water flow model, in *Techniques of Water Resources Evaluations*, book 6, chapter A1, U.S.Geological Survey.

Schulenberg, J.W. and Reeves, H.W. (2002) Axi-symmetric simulation of soil vapor extraction influenced by soil fracturing. *Journal of Contaminant Hydrology* **57**, 189-222.

Tenney, C.M, Lastoskie, C.M. and Dybas, M.J. A reactor model for trap-and-treat groundwater remediation. *Water Research*, submitted and in review.

Voudrias, E.A. and Yeh, M.F. (1994) Dissolution of a toluene pool under constant and variable hydraulic gradients with implications for aquifer remediation. *Ground Water* **32**, 305-311.

Whelan, M.P., Voudrias, E.A. and Pearce, A. (1994) DNAPL pool dissolution in saturated porous media: procedure development and preliminary results. *Journal of Contaminant Hydrology* **15**, 223-237.

Zhang, H., Baray, D.A. and Hocking, G.C. (1999) Analysis of continuous and pulsed pumping of a phreatic aquifer. *Advances in Water Resources* **22**, 623-632.

Zheng, C. (1992) MT3D: A modular three-dimensional transport model, in *Documentation and User's Guide*, S.S. Papadopulos & Associates, Inc.